Prognostic model for predicting overall survival in children and adolescents with rhabdomyosarcoma.	Yang L, Takimoto T, Fujimoto J.	BMC Cancer. 14:654-60	2014	国外
Clinical initiatives linking Japanese and Swedish healthcare resources on cancer studies utilizing Biobank Repositories.	Nishimura T, Kawamura T, Sugihara Y, Bando Y, Sakamoto S, Nomura M, Ikeda N, Ohira T, Fujimoto J, Tojo H, Hamakubo T, Kodama T, Andersson R, Fehniger TE, Kato H, Marko-Varga G.	Clin Transl Med. 3:38-42	2014	国外
Statistical analysis of relation between plasma methotrexate concentration and toxicity in high-dose methotrexate therapy of childhood nonHodgkin lymphoma.	Tsurusawa M, Gosho M, Mori T, Mitsui T, Sunami S, Kobayashi R, Fukano R, Tanaka F, Fujita N, Inada H, Koh K, Takimoto T, Saito A, Fujimoto J, Nakazawa A, Horibe K.	Pediatr Blood Cancer	in press, 2015	国外

Ⅴ．研究成果の代表的論文

Int J Hematol (2014) 99:154–161
DOI 10.1007/s12185-013-1487-5

ORIGINAL ARTICLE

Liver disease is frequently observed in Down syndrome patients with transient abnormal myelopoiesis

Myoung Ja Park · Manabu Sotomatsu · Kentaro Ohki · Kokoro Arai · Kenichi Maruyama · Tomio Kobayashi · Akira Nishi · Kiyoko Sameshima · Takeshi Takagi · Yasuhide Hayashi

Received: 1 August 2013 / Revised: 26 November 2013 / Accepted: 26 November 2013 / Published online: 14 December 2013

Abstract Transient abnormal myelopoiesis (TAM) in neonates with Down syndrome (DS) is characterized by the transient appearance of blast cells, which resolves spontaneously. Approximately 20 % of patients with TAM die at an early age due to organ failure, including liver disease. We studied 25 DS-TAM patients retrospectively to clarify the correlation between clinical and laboratory characteristics and liver diseases. Early death (<6 months of age) occurred in four of the 25 patients (16.0 %), and two of those four patients died due to liver failure. Although physiologic jaundice improved gradually after a week, all DS patients had elevated D-Bil levels during the clinical course of TAM, except one who suffered early death. The median peak day of the WBC count, total bilirubin (T-Bil) and D-Bil levels was: day 1 (range day 0–57), day 8 (range day 1–55), and day 17 (range 1–53), respectively. Our results reveal that all patients with DS-TAM may develop liver disease irrespective of the absence or presence of symptoms and risk factors for early death. In patients of DS-TAM, careful observation of the level of D-Bil is needed by at least 1 month of age for the detection of liver disease risk.

Keywords Down syndrome · AML · Liver disease · Direct bilirubin · Cytarabine therapy

M. J. Park (✉) · M. Sotomatsu · K. Ohki · K. Arai · Y. Hayashi
Department of Hematology/Oncology, Gunma Children's Medical Center, 779 Shimohakoda, Hokkitsu, Shibukawa, Gunma 377-8577, Japan
e-mail: pakum-tky@umin.ac.jp

K. Maruyama
Department of Neonatology, Gunma Children's Medical Center, Gunma, Japan

T. Kobayashi
Department of Cardiology, Gunma Children's Medical Center, Gunma, Japan

A. Nishi
Department of Pediatric Surgery, Gunma Children's Medical Center, Gunma, Japan

K. Sameshima
Department of Genetics, Gunma Children's Medical Center, Gunma, Japan

T. Takagi
Department of Obstetrics, Gunma Children's Medical Center, Gunma, Japan

Introduction

Down syndrome (DS), or constitutional trisomy 21, is the most common human aneuploidy with an incidence of 1 in 700 births [1]. About 10 % of neonates with DS exhibit unique clonal myeloproliferation characterized by immature megakaryoblasts in the fetal liver and peripheral blood (PB) [2–4]. The first case was reported as transient leukemia, and this hematological abnormality is also known as transient myeloproliferative disorder [5, 6]. In the 2008 version of the World Health Organization classification, it was referred to as myeloid proliferations related to DS, 'transient abnormal myelopoiesis' (TAM) [7, 8]. Although megakaryoblasts spontaneously regress in most patients by the age of 3 months, it is regarded as a pre-leukemic syndrome; approximately 20 % of children diagnosed with TAM develop acute megakaryoblastic leukemia (AMKL) within 4 years [6, 9, 10].

The majority of affected neonates with DS may be asymptomatic other than an elevated WBC count or

hepatomegaly [11, 12]. TAM infrequently presents as hydrops fetalis in utero, but is commonly diagnosed during the first week after birth [12, 13]. Approximately 20 % of TAM patients die at an early age due to organ failure, including liver disease [9, 12, 14]. According to previous reports, early death was correlated with a higher WBC count, ascites, preterm delivery, bleeding diatheses, failure of spontaneous remission, and elevated direct bilirubin (D-Bil) levels [9, 12, 14].

Jaundice, the visible sign of hyperbilirubinemia, is more common in infancy than at any other time of life. Physiologic jaundice is the most common cause of neonatal jaundice. In general, there are some criteria to help distinguish physiologic jaundice from pathologic jaundice in neonates. These included: (1) jaundice prior to 36 h of age, (2) a serum total bilirubin (T-Bil) level above 12 mg/dl, (3) persistent jaundice beyond the eighth day of life, and (4) D-Bil fraction is >2 mg/dl at any time [15, 16].

Cholestasis affects approximately 1 in every 2,500 infants and is an infrequent but potentially serious condition that indicates liver dysfunction [17, 18]. Since hyperbilirubinemia may be present in an infant who does not appear acutely ill, the measurement of D-Bil or conjugated bilirubin level is recommended [19, 20]. The potential cause of cholestasis in neonates is diverse; therefore, it is important to recognize specific treatable metabolic or infectious diseases and establish early, appropriate, and effective management. Every infant presenting with jaundice beyond the age of 2 weeks should be evaluated with fractionated bilirubin to exclude life-threatening conditions or disorders requiring urgent specific treatment [21].

A prospective study reported that 21 % of TAM patients developed the symptoms of cholestasis or elevated liver enzymes [12]. TAM is sometimes complicated by liver fibrosis, which is life-threatening and often fatal [22–25]. However, the precise frequency of liver fibrosis is not known. The infiltration of megakaryoblasts with liver fibrosis has been shown histologically [22, 23]. The DS-TAM patients with liver fibrosis will be progressive and fatal [24, 26].

Elevated D-Bil levels are a sign of serious liver disease in infants with TAM [6]. However, the detailed clinical characteristics of TAM with liver disease remain unclear. We studied 25 DS-TAM patients in our hospital retrospectively to clarify the correlation between clinical and laboratory characteristics and liver diseases.

Methods

A retrospective chart review of patients admitted to Gunma Children's Medical Center in Japan between January 2001 and June 2012 was undertaken to identify the characteristics of liver disease in DS infants with TAM. Morphologic evidence of myeloid blasts in the PB was confirmed in all eligible patients. The eligibility criteria for this analysis were DS infants who were younger than 3 months. Patients with leukocytosis and peripheral blast cells as a result of infections or other causes were excluded. Elevated D-Bil levels were defined as D-Bil level $\geq$ 1.5 mg/dl [15, 16, 20]. Here we defined conjugated hyperbilirubinemia as D-Bil $\geq$ 2 mg/dl. Although the terms D-Bil are used equivalently with conjugated bilirubin in the reviews [16], this is no quantitatively correct, because the direct fraction includes both conjugated bilirubin and delta bilirubin [19]. It has been reported that the 99th percentile for D-Bil is 2.1 mg/dl in the retrospective study of a birth cohort of 271,186 full-term newborns including 259 DS infants [27]. D-Bil fraction $\geq$2 mg/dl at any time is pathological jaundice in neonate, whether the patient is Down syndrome or not, that indicates the possibility of cholestasis. Cholestasis is defined physiologically as reduction in bile flow and morphologically as the presence of bile pigment in histologic sections of liver [16]. This study was approved by the Ethics Committee of our hospital, and written informed consent was obtained from all parents.

Results

The clinical characteristics of TAM patients are summarized in Table 1. The 25 patients in this study included 13 males and 12 females. The median gestational age and birth weight were 37 weeks (range 32–41 weeks) and 2,600 g (range 1,622–3,552 g), respectively. The median age at diagnosis was 0 days, with a range from 0 to 28 days. Congenital cardiac abnormalities were seen in 21 (84.0 %) of 25 patients. Elevated D-Bil levels were found in 24 (96.0 %) of 25 patients, systemic edema in 5 (20.0 %) of 25, and disseminated intravascular coagulation (DIC) in 5 (20.0 %) of 25, respectively. Among the 25 patients requiring therapeutic intervention, 6 received exchange blood transfusion, 5 received steroid therapy, and 3 received a low dose of cytarabine. Early death (<6 months of age) occurred in 4 (16.0 %) of 25 patients and the median age at death was 50 days (range 1–156 days). Two of the 4 patients were born with hydrops fetalis and died at day 1 and 44 due to multiorgan failure. The other 2 patients died because of liver failure. Six patients (24.0 %) developed AMKL.

The laboratory findings of 25 patients are summarized in Table 2. The median WBC count and percentage of blasts in the PB at diagnosis were 30,600/μl (range 4,600–183,000/μl) and 36 % (range 2–96 %), respectively. The median peak day of the WBC count, and T-Bil and

Table 1 Clinical findings in 25 TAM cases

Patient number	Gender	Gestational age (weeks)	Birth weight (g)	Age at diagnosis (day)	Congenital abnormalies	Cholestatic jaundice	Systemic edema	DIC	Therapeutic intervention	Outcome	AMKL
1	F	35	2,710	0	VSD	−	+	+	−	Dead at day 1	−
2	M	37	2,958	0	PDA, ASD, VSD	+	+	−	PSL, ET, AraC	Alive	−
3	M	40	3,552	0	PDA, ASD, VSD	+	−	+	PSL	Dead at day 609	−
4	F	39	2,884	0	PDA, ASD, VSD	+	−	−	−	Alive	−
5	F	37	2,870	0	PDA, ASD, VSD	+	−	+	ET	Alive	+
6	M	35	2,680	16	PDA, ASD, VSD	+	−	−	−	Alive	−
7	M	38	2,600	0	VSD	+	−	−	−	Alive	−
8	M	38	3,282	0	PDA	+	−	+	−	Dead at day 1,217	+
9	M	37	2,252	25	−	+	−	−	PSL, ET, AraC	Dead at day 156	−
10	M	34	2,038	28	PDA, TOF	+	−	−	−	Alive	−
11	F	38	2,626	7	PDA	+	−	−	−	Alive	−
12	F	32	1,622	0	−	+	−	−	−	Alive	+
13	F	32	2,122	0	ASD	+	+	−	−	Dead at 399	−
14	F	34	2,510	21	PDA, ASD	+	+	−	ET	Dead at day 44	−
15	M	36	2,128	0	PDA, ASD	+	−	−	−	Alive	+
16	F	36	2,150	0	−	+	+	+	PSL, ET	Dead at day 55	−
17	F	36	2,059	0	ASD,VSD	+	−	−	−	Alive	−
18	M	41	2,726	0	ASD, VSD	+	−	−	PSL, ET, AraC	Alive	−
19	M	39	2,515	0	ASD, VSD	+	−	−	−	Alive	−
20	M	35	2,890	1	−	+	−	−	−	Alive	−
21	F	36	1,992	3	PDA, VSD	+	−	−	−	Alive	+
22	F	37	2,802	0	ASD, VSD, TOF	+	−	−	−	Alive	−
23	M	34	2,058	3	PDA	+	−	−	−	Alive	+
24	F	37	2,554	0	PDA, VSD	+	−	−	−	Alive	−
25	M	39	2,870	8	PDA	+	−	−	−	Alive	−

ASD atrial septal defect, *VSD* ventricular septal defec, *TOF* tetralogy of Fallot, *PDA* patent ductus arteriosus, *PSL* prednisolone, *ET* exchange blood transfusion, *AraC* cytarabine

D-Bil levels were day 1 (range day 0–57), day 8 (range day 1–55), and day 17 (range 1–53), respectively. All 24 patients except one suffered from early death showed D-Bil levels above 1.5 mg/dl, and 19 (76.0 %) of 25 patients showed D-Bil levels above 2.0 mg/dl with or without the symptoms of liver failure. The median first day of D-Bil levels over 1.5 and 2.0 mg/dl was day 10 (range day 1–28) and day 14 (range day 0–32), respectively. Liver biopsy was performed in 3 patients with the symptoms of liver failure. The pathological diagnosis of patient 6 was non-syndromic paucity of interlobular bile ducts (NS-PILBD).

The correlation between patient covariates and conjugated hyperbilirubinemia (D-Bil $\geq$ 2 mg/dl) is shown in Table 3. Conjugated hyperbilirubinemia was not significantly associated with gender, birth weight, gestational age, DIC, systemic edema, or a higher WBC count. The

Table 2 Laboratory findings in 25 TAM cases

Patient number	WBC count at diagnosis (/μl)	PB blasts (%)	Platelet ($\times 10^3$/μl)	Peak value of WBC (/μl)	Day of peak WBC	Peak value of T-Bil (mg/dL)	Day of peak T-Bil	Peak value of D-Bil (mg/dL)	Day of peak D-Bil	Day of D-Bil ≥2 mg/dl	Day of D-Bil ≥1.5 mg/dl	Peak value of AST	Peak value of ALT
1	21,300	15	147.0	21,300	0	2.13	1	0.83	1	–	–	254	88
2	12,900	11	210.0	15,300	0	16.32	8	9.47	31	8	2	116	96
3	72,600	53	26.0	72,600	0	12.56	6	2.28	13	13	10	73	126
4	89,400	64	429.0	89,400	0	26.84	11	3.08	23	12	12	102	163
5	183,000	88	665.0	183,000	0	7.12	3	3.14	4	3	1	265	67
6	12,000	4	178.0	13,000	0	23.76	16	6.46	34	16	16	430	374
7	14,500	39	66.0	21,800	2	5.62	3	1.61	1	–	1	50	10
8	74,100	36	162.0	91,200	1	16.33	6	2.36	1	1	1	45	34
9	7,700	22	56.0	7,700	25	29.50	43	18.98	42	25	25	303	125
10	17,200	40	79.0	40,100	57	7.83	28	2.4	29	29	28	48	18
11	30,700	77	83.0	31,900	15	12.28	8	2.4	15	15	15	22	14
12	25,000	50	136.0	25,000	0	12.31	9	3.93	14	14	14	66	24
13	26,000	49	121.0	35,100	1	13.36	9	2.1	4	4	4	785	183
14	114,000	96	4.7	138,000	42	6.49	36	5.97	42	24	24	121	24
15	181,900	87	925.0	183,000	2	12.60	2	1.73	5	–	0	136	179
16	46,200	53	293.0	74,400	21	46.97	55	18.72	53	2	2	214	71
17	32,300	22	59.0	32,300	0	12.56	6	2.8	20	15	1	43	50
18	118,900	89	310.0	118,900	0	13.20	5	3.18	32	32	18	28	21
19	19,500	4	230.0	23,200	2	15.23	2	4.18	10	4	0	105	97
20	41,800	30	241.0	48,900	2	4.10	16	1.92	17	–	4	37	46
21	6,400	6	66.0	10,300	3	13.26	7	2.14	15	15	1	70	76
22	16,400	9	250.0	23,000	1	13.63	6	1.85	14	–	14	39	16
23	36,700	32	960.0	36,700	0	16.18	16	2.12	27	27	27	50	83
24	30,600	6	36.0	35,000	1	17.75	9	1.96	20	–	20	37	10
25	4,600	2	69.0	6,800	46	10.13	8	2.62	20	11	10	88	18

WBC white blood cell, *PB* peripheral blood, *T-Bil* total bilirubin, *D-Bil* direct bilirubin

correlation between patient covariates and early death is shown in Table 4. Early death was significantly associated with a peak D-Bil level of greater than 5 mg/dl ($p = 0.016$).

Five representative patients with marked cholestatic jaundice are described below. The T-Bil and D-Bil levels, WBC count, and blast ratio in the PB of 4 patients are shown in Fig. 1. Figure 1a shows the clinical course of patient 2. He exhibited hydrops fetalis at birth. T-Bil and D-Bil levels at birth were 5.99 and 1.07 mg/dl, respectively. His serum markers of liver fibrosis were high: procollagen Type III Peptide (P-III-P) was 9.7 U/ml (normal range 0.3–0.8 U/ml) and type IV collagen was 1,019 ng/ml (normal range <150 ng/ml). D-Bil levels over 1.5 and 2.0 mg/dl occurred on day 2 and day 8, respectively. After 1 week, the D-Bil level gradually increased while the T-Bil level concomitantly decreased. Although therapeutic intervention was started with steroids and a low dose of cytarabine, the D-Bil level still increased. A liver biopsy was performed to clarify the cause of pathological jaundice. The histopathological findings were mild liver fibrosis without leukemic cell infiltration. After exchange blood transfusion was performed on day 40, pathological jaundice improved.

Patient 9 was admitted to our hospital on day 25 because of jaundice. T-Bil and D-Bil levels at diagnosis were 19.76 and 13.11 mg/dl, respectively. After admission, T-Bil and D-Bil levels gradually increased. Despite therapeutic intervention by exchange blood transfusion, steroids, and a low dose of cytarabine, the patient died on day 156 because of liver failure. Although he received the operation for imperforate anus on day 1, TAM was not diagnosed. The WBC count on day 1 in previous hospital was 7,400/μl and blast in PB was not noticed.

Patient 16 was admitted on day 0 because of congenital jejunal atresia. T-Bil and D-Bil levels at diagnosis were 9.14 and 2.04 mg/dl, respectively. After jejunostomy, the D-Bil level decreased to below normal levels, and then gradually increased again in spite of therapeutic intervention by exchange blood transfusion. The patient died on day 55 because of liver failure. Liver histology showed severe liver fibrosis without leukemic cell infiltration.

Patient 17 was admitted to our hospital because of congenital heart disease. Initial T-Bil and D-Bil levels were

Table 3 Correlation between patient covariates and conjugated hyperbilirubinemia (D-Bil ≧ 2 mg/dl)

	Patients with conjugated hyperbilirubinemia	Patients without conjugated hyperbilirubinemia	Total patients	*p*
Gender				
Male	10	3	13	1
Female	9	3	12	
Birth weight				
Birth weight ≧2.5 kg	11	5	16	0.364
Birth weight <2.5 kg	8	1	9	
Gestational age				
Term ≧37 weeks	10	3	13	1
Preterm <37	9	3	12	
Systemic edema				
+	4	1	5	1
−	15	5	20	
DIC				
+	4	1	5	1
−	15	5	20	
WBC at diagnosis				
WBC ≧10 × 10^4/μl	3	1	4	1
WBC <10 × 10^4/μl	16	5	21	

p value (Fisher's test)

Table 4 Correlation between clinical data and early death

	Patients with EA	Patients without EA	Total patients	*p*
Gender				
Male	1	12	13	0.322
Female	3	9	12	
Birth weight				
Birth weight ≧2.5 kg	2	14	16	0.602
Birth weight <2.5 kg	2	7	9	
Gestational age				
Term ≧37 weeks	1	12	13	0.322
Preterm <37 weeks	3	9	12	
WBC at diagnosis				
WBC ≧100 × 10^3/μl	1	3	4	0.527
WBC <100 × 10^3/μl	3	18	21	
Peak value of D-Bil				
D-Bil ≧5 mg/dl	3	2	5	0.016
D-Bil <5 mg/dl	1	19	20	

EA early death (<6 months of age), *p* value (Fisher's test)

2.34 and 0.87 mg/dl, respectively. The D-Bil level gradually increased from day 15, while the T-Bil level adversely decreased. Megakaryoblasts regressed spontaneously on day 13 and the D-Bil level decreased from day 24 without therapeutic intervention. Her serum markers of liver fibrosis were high from birth: P-III-P was 8.1 U/ml and type IV collagen was 1,040 ng/ml. In this patient, the D-Bil level was above 2 mg/dl and high levels of P-III-P and type IV collagen were observed, but cholestatic symptoms were not apparent.

Patient 19 was admitted to our hospital because of congenital heart disease. Initial T-Bil and D-Bil levels were 5.47 and 1.97 mg/dl, respectively. The level of D-Bil increased from day 4, while the T-Bil level adversely decreased. Therapeutic intervention by steroids was started on day 30. Thereafter, the D-Bil level decreased, and banding therapy for patent ductus arteriosus (PDA) was performed on day 50. Her serum markers of liver fibrosis were P-III-P (17.5 U/ml) and type IV collagen (948 ng/ml).

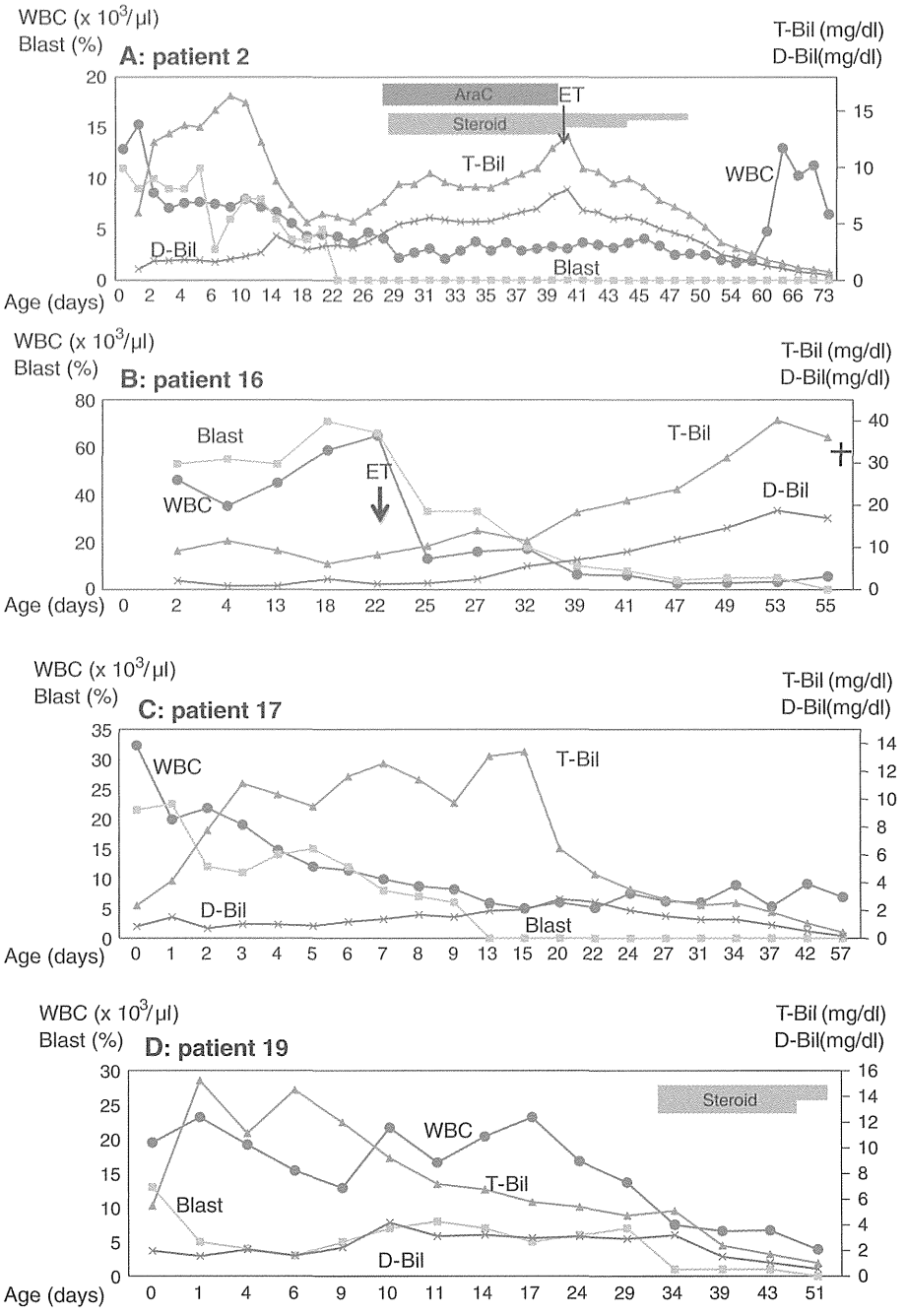

Fig. 1 T-Bil and D-Bil levels, WBC count, and blast ratio in PB of 4 patients (**a** patient 2, **b** patient 16, **c** patient 17, **d** patient 19). *ET* exchange blood transfusion

Discussion

We studied 25 DS-TAM patients retrospectively to clarify the correlation between clinical and laboratory characteristics and liver diseases. Two of 4 patients died within 6 months after birth due to liver failure. Three of 5 patients with D-Bil levels greater than 5 mg/dl died early due to multiorgan failure. Early death was associated with a peak D-Bil level greater than 5 mg/dl ($p = 0.016$). Our result was similar to previous studies [9, 12, 14], but the number of our study was small.

Although our study is retrospective in single institution, we showed that liver disease could occur in DS patients without any risk factor of early death even after the disappearance or decrease of blast cells in PB. In our study, the median first day of D-Bil levels over 1.5 mg/dl and 2.0 mg/dl was day 10 (range day 1–28) and day 14 (range day 0–32), respectively. Although physiologic jaundice improved gradually 1 week after birth, the level of D-Bil adversely increased in all DS patients with TAM. All DS patients had elevated D-Bil levels regardless of the risk for early death during the clinical course of TAM. The level of

D-Bil is one of the most reliable markers in TAM accompanied by liver disease. It is necessary to monitor the level of D-Bil in DS-TAM patients, and careful attention is needed not to exceed above 2 mg/dl.

The precise frequency of TAM is unknown because no large population-based study among patients has been carried out to verify it yet [9]. If the diagnosis of TAM has not been made due to the lack of symptoms within 1 week after birth, similar to patient 9, the TAM patients may already have uncorrectable liver disease at presentation. An urgent referral is considered to be necessary for further diagnostic investigations in patients of elevated D-Bil levels as previously reported [28].

Although the clinical manifestations of neonatal cholestasis are usually similar, they may include potentially serious disorders. However, identifying these neonates with cholestasis from lots of patients with physiologic jaundice can be difficult. As shown in patient 2, T-Bil is not a reliable marker of cholestasis. For this reason, conjugated bilirubin and D-Bil levels are often measured. D-Bil measurement estimates the total concentration of the conjugated and delta bilirubin. False positive results have been reported to be less likely when using conjugated bilirubin levels than when using D-Bil levels in assessment of the biliary disease in newborn [27]. Conjugated bilirubin and D-Bil level measurement may be the prognostic factors to predict severe liver disease in TAM patients.

Differential diagnoses among biliary atresia, idiopathic neonatal hepatitis, and intrahepatic cholestasis are particularly difficult to make. Liver biopsy provides the highest diagnostic usefulness in neonatal cholestasis [28]. Using liver biopsy, we diagnosed NS-PILBD in a cholestatic patient with TAM [29]. Biliary atresia in a DS patient has also been reported [30]. Liver biopsy may allow the differential diagnosis of cholestasis and provide additional information such as the presence of megakaryoblasts in the liver and the severity of liver fibrosis.

The treatment of liver disease in TAM has not yet been established. Hepatic synthetic dysfunction leads to bleeding and it is important to ascertain the cause of bleeding and management of patients who have TAM with liver disease. Medical management is mainly supportive and aims for optimal growth, development, and the treatment of complications such as fat malabsorption, fat-soluble vitamin deficiencies, cirrhosis, portal hypertension, and liver failure [21]. The administration of vitamin K is needed for the initial treatment of cholestatic infants to prevent hemorrhage. The decreased delivery of bile acids to the proximal intestine leads to the inadequate digestion and absorption of dietary long-chain triglycerides and fat-soluble vitamins. Infant formulas containing medium chain triglycerides (MCTs) provide better energy balance. Ursodeoxycholic acid (20 mg/kg/day) may also be effective in encouraging bile flow and bile drainage [31].

It has been reported that treatment with cytarabine (0.5–1.5 mg/kg) has a beneficial effect on the outcome of TAM with high risk factors for early death [12]. In our study, three of 25 patients were treated with a low dose of cytarabine, and D-Bil and transaminases levels increased after cytarabine therapy in patients 2 and 9. It is not certain whether a low dose of cytarabine is effective in TAM patients with liver dysfunction after the disappearance of blast cells in PB. Liver disease in DS-TAM progresses even if blast cells disappear. No therapy is known to be effective in inhibiting the progression of cholestasis or preventing further hepatocellular damage and cirrhosis. Thus, we emphasize that the early detection of DS-TAM patients with liver disease is very important. As shown in patient 16, the percentage of blasts in PB is not related to liver disease, and careful observation of D-Bil or conjugated bilirubin levels was needed at least 1 month of age in DS-TAM.

Another strategy may be to inhibit fibroblastic proliferation with a biological response modifier such as a steroid. The clinical course of patient 19 suggested that some TAM patients with liver disease may benefit from steroid therapy. Cytokines have been reported to be produced by blast cells such as platelet-derived growth factor and transforming growth factor B, and may play an important role in the progression of cholestasis [32–34]. It has been also reported that blasts and liver tissue from TAM patients with hepatic fibrosis showed a significantly elevated expression of PDGF gene [33]. Some DS-TAM patient with liver disease may improve without therapeutic intervention, as patient 17. Treatment with steroids and exchange blood transfusion may be effective in reducing the cytokine storm before serious liver damage can occur.

In summary, we retrospectively studied 25 DS-TAM patients to identify a correlation between clinical and laboratory characteristics and liver diseases. Our results revealed that all patients with DS-TAM have potential liver disease regardless of the existence of symptoms and risk factors for early death. In patients of DS-TAM, careful observation of the level of D-Bil or conjugated bilirubin is needed at least until 1 month of age for liver disease.

Acknowledgments This work was supported by a grant for Cancer Research, and a grant for Research on Children and Families from the Ministry of Health, Labor, and Welfare of Japan, and a Grant-in-Aid for Scientific Research (B) and (C) and Exploratory Research from the Ministry of Education, Culture, Sports, Science, and Technology of Japan, and a Research grant for Bureau of Gunma Prefectural Hospitals.

References

1. Malinge S, Izraeli S, Crispino JD. Insights into the manifestations, outcomes, and mechanisms of leukemogenesis in Down syndrome. Blood. 2009;113:2619–28.
2. Pine SR, Guo Q, Yin C, Jayabose S, Druschel CM, Sandoval C. Incidence and clinical implications of GATA1 mutations in newborns with Down syndrome. Blood. 2007;110:2128–31.
3. Zipursky A, Brown EJ, Christensen H, Doyle J. Transient myeloproliferative disorder (transient leukemia) and hematologic manifestations of Down syndrome. Clin Lab Med. 1999;19: 157–67.
4. Bajwa RP, Skinner R, Windebank KP, Reid MM. Demographic study of leukaemia presenting within the first 3 months of life in the Northern Health Region of England. J Clin Pathol. 2004;57:186–8.
5. Schunk GJ, Lehman WL. Mongolism and congenital leukemia. J Am Med Assoc. 1954;155:250–1.
6. Lange B. The management of neoplastic disorders of haematopoiesis in children with Down's syndrome. Br J Haematol. 2000;110:512–24.
7. Nagao T, Lampkin BC, Hug G. A neonate with Down's syndrome and transient abnormal myelopoiesis: serial blood and bone marrow studies. Blood. 1970;36:443–7.
8. Vardiman JW, Thiele J, Arber DA, Brunning RD, Borowitz MJ, Porwit A, et al. The 2008 revision of the World Health Organization (WHO) classification of myeloid neoplasms and acute leukemia: rationale and important changes. Blood. 2009;114: 937–51.
9. Massey GV, Zipursky A, Chang MN, Doyle JJ, Nasim S, Taub JW, et al. A prospective study of the natural history of transient leukemia (TL) in neonates with Down syndrome (DS): Children's Oncology Group (COG) study POG-9481. Blood. 2006;107: 4606–13.
10. Homans AC, Verissimo AM, Vlacha V. Transient abnormal myelopoiesis of infancy associated with trisomy 21. Am J Pediatr Hematol Oncol. 1993;15:392–9.
11. Zipursky A. Transient leukaemia—a benign form of leukaemia in newborn infants with trisomy 21. Br J Haematol. 2003;120: 930–8.
12. Klusmann JH, Creutzig U, Zimmermann M, Dworzak M, Jorch N, Langebrake C, et al. Treatment and prognostic impact of transient leukemia in neonates with Down syndrome. Blood. 2008;111:2991–8.
13. Zipursky A, Rose T, Skidmore M, Thorner P, Doyle J. Hydrops fetalis and neonatal leukemia in Down syndrome. Pediatr Hematol Oncol. 1996;13:81–7.
14. Muramatsu H, Kato K, Watanabe N, Matsumoto K, Nakamura T, Horikoshi Y, et al. Risk factors for early death in neonates with Down syndrome and transient leukaemia. Br J Haematol. 2008;142:610–5.
15. Ambalavanan N, Carlo WA. Jaundice and hyperbilirubinemia in the Newborn. In: Kligman RM, Stanton BF, Geme JS, Scgor NF, editors. Nelson textbook of pediatrics. Philadelphia: Elsevier; 2011. p. 603–5.
16. Mathis RK, Andres JM, Walker WA. Liver disease in infants. Part II: hepatic disease states. J Pediatr. 1977;90:864–80.
17. Dick MC, Mowat AP. Hepatitis syndrome in infancy–an epidemiological survey with 10 year follow up. Arch Dis Child. 1985;60:512–6.
18. Balistreri WF. Neonatal cholestasis. J Pediatr. 1985;106:171–84.
19. Brumbaugh D, Mack C. Conjugated hyperbilirubinemia in children. Pediatr Rev. 2012;33:291–302.
20. Moyer V, Freese DK, Whitington PF, Olson AD, Brewer F, Colletti RB, et al. Guideline for the evaluation of cholestatic jaundice in infants: recommendations of the North American Society for Pediatric Gastroenterology, Hepatology and Nutrition. J Pediatr Gastroenterol Nutr. 2004;39:115–28.
21. McKiernan PJ. Neonatal cholestasis. Semin Neonatol. 2002;7: 153–65.
22. Becroft DM, Zwi LJ. Perinatal visceral fibrosis accompanying the megakaryoblastic leukemoid reaction of Down syndrome. Pediatr Pathol. 1990;10:397–406.
23. Ruchelli ED, Uri A, Dimmick JE, Bove KE, Huff DS, Duncan LM, et al. Severe perinatal liver disease and Down syndrome: an apparent relationship. Hum Pathol. 1991;22:1274–80.
24. Miyauchi J, Ito Y, Kawano T, Tsunematsu Y, Shimizu K. Unusual diffuse liver fibrosis accompanying transient myeloproliferative disorder in Down's syndrome: a report of four autopsy cases and proposal of a hypothesis. Blood. 1992;80:1521–7.
25. Schwab M, Niemeyer C, Schwarzer U. Down syndrome, transient myeloproliferative disorder, and infantile liver fibrosis. Med Pediatr Oncol. 1998;31:159–65.
26. Al-Kasim F, Doyle JJ, Massey GV, Weinstein HJ, Zipursky A. Incidence and treatment of potentially lethal diseases in transient leukemia of Down syndrome: Pediatric Oncology Group Study. J Pediatr Hematol Oncol. 2002;24:9–13.
27. Davis AR, Rosenthal P, Escobar GJ, Newman TB. Interpreting conjugated bilirubin levels in newborns. J Pediatr. 2011; 158(562–5):e1.
28. De Bruyne R, Van Biervliet S, Vande Velde S, Van Winckel M. Clinical practice: neonatal cholestasis. Eur J Pediatr. 2011;170: 279–84.
29. Sotomatsu M, Park MJ, Shimada A, hayashi Y. A case of Down syndrome with transient abnormal myelopoiesis and nonsyndromic paucity of interlobular bile ducts. Jpn J Pediatric Hematol. 2008;22:34–7.
30. Puri P, Guiney EJ. Intrahepatic biliary atresia in Down's syndrome. J Pediatr Surg. 1975;10:423–4.
31. Kelly DA, Davenport M. Current management of biliary atresia. Arch Dis Child. 2007;92:1132–5.
32. Terui T, Niitsu Y, Mahara K, Fujisaki Y, Urushizaki Y, Mogi Y, et al. The production of transforming growth factor-beta in acute megakaryoblastic leukemia and its possible implications in myelofibrosis. Blood. 1990;75:1540–8.
33. Hattori H, Matsuzaki A, Suminoe A, Ihara K, Nakayama H, Hara T. High expression of platelet-derived growth factor and transforming growth factor-beta 1 in blast cells from patients with Down syndrome suffering from transient myeloproliferative disorder and organ fibrosis. Br J Haematol. 2001;115:472–5.
34. Shimada A, Hayashi Y, Ogasawara M, Park MJ, Katoh M, Minakami H, et al. Pro-inflammatory cytokinemia is frequently found in Down syndrome patients with hematological disorders. Leuk Res. 2007;31:1199–203.

nature COMMUNICATIONS

ARTICLE

Received 29 Jan 2014 | Accepted 21 Jul 2014 | Published 27 Aug 2014

DOI: 10.1038/ncomms5770

Recurrent *CDC25C* mutations drive malignant transformation in FPD/AML

Akihide Yoshimi[1,*], Takashi Toya[1,*], Masahito Kawazu[2], Toshihide Ueno[3], Ayato Tsukamoto[1], Hiromitsu Iizuka[1], Masahiro Nakagawa[1], Yasuhito Nannya[1], Shunya Arai[1], Hironori Harada[4], Kensuke Usuki[5], Yasuhide Hayashi[6], Etsuro Ito[7], Keita Kirito[8], Hideaki Nakajima[9], Motoshi Ichikawa[1], Hiroyuki Mano[3] & Mineo Kurokawa[1]

Familial platelet disorder (FPD) with predisposition to acute myelogenous leukaemia (AML) is characterized by platelet defects with a propensity for the development of haematological malignancies. Its molecular pathogenesis is poorly understood, except for the role of germline *RUNX1* mutations. Here we show that *CDC25C* mutations are frequently found in FPD/AML patients (53%). Mutated CDC25C disrupts the G2/M checkpoint and promotes cell cycle progression even in the presence of DNA damage, suggesting a critical role for CDC25C in malignant transformation in FPD/AML. The predicted hierarchical architecture shows that *CDC25C* mutations define a founding pre-leukaemic clone, followed by stepwise acquisition of subclonal mutations that contribute to leukaemia progression. In three of seven individuals with *CDC25C* mutations, *GATA2* is the target of subsequent mutation. Thus, *CDC25C* is a novel gene target identified in haematological malignancies. *CDC25C* is also useful as a clinical biomarker that predicts progression of FPD/AML in the early stage.

[1] Department of Hematology and Oncology, Graduate School of Medicine, The University of Tokyo, 7-3-1 Hongo, Bunkyo-ku, Tokyo 113-8655, Japan. [2] Department of Medical Genomics, Graduate School of Medicine, The University of Tokyo, 7-3-1 Hongo, Bunkyo-ku, Tokyo 113-8655, Japan. [3] Department of Cellular Signaling, Graduate School of Medicine, The University of Tokyo, 7-3-1 Hongo, Bunkyo-ku, Tokyo 113-8655, Japan. [4] Department of Hematology, Juntendo University School of Medicine, 3-1-3 Hongo, Bunkyo-ku, Tokyo 113-8431, Japan. [5] Department of Hematology, NTT Medical Center Tokyo, 5-9-22 Higashi-Gotanda, Shinagawa-ku, Tokyo 141-8625, Japan. [6] Department of Hematology/Oncology, Gunma Children's Medical Center, 779 Simohakoda, Kitaakebonocho, Shibukawa-shi, Gunma 377-8577, Japan. [7] Department of Pediatrics, Graduate School of Medicine, Hirosaki University, 53 Honmachi, Hirosaki-shi, Aomori 036-8563, Japan. [8] Department of Hematology and Oncology, University of Yamanashi, 1110 Simokawakita, Chuou-shi, Yamanashi 409-3898, Japan. [9] Division of Hematology, Department of Internal Medicine, Keio University School of Medicine, 35 Shinanomachi, Shinjyuku-ku, Tokyo 160-8582, Japan. * These authors contributed equally to this work. Correspondence and requests for materials should be addressed to M.K. (email: kurokawa-tky@umin.ac.jp).

Familial platelet disorder (FPD)/acute myelogenous leukaemia (AML) (MIM601399) is an autosomal dominant disorder with inherited thrombocytopenia, abnormal platelet function and a lifelong risk of the development of a variety of haematological malignancies[1], such as AML, myelodysplastic syndromes (MDS) and myeloproliferative neoplasms. Although inherited *RUNX1* mutations are the cause of the congenital thrombocytopenia, it remains unclear whether a mutation in *RUNX1*, which is generally known to have a dominant-negative effect[2–4], is sufficient to induce the development of haematological malignancies in individuals with FPD/AML. It is also not known whether additional gene mutations are required for the transformation, and, if so, which genes are involved. Given that only 40% of FPD/AML patients develop these neoplasms[5] and that a relatively long period is required for subsequent *RUNX1* mutation-mediated development of neoplasms in FPD/AML, the secondary genetic events may function as a driver to promote malignant transformation. We reasoned that identifying gene mutations responsible for the malignant transformation of FPD/AML would provide indispensable information for addressing these questions. However, only about 30 pedigrees with FPD/AML have been reported so far, and the rarity of this disorder has impeded the establishment of clinical diagnostic criteria and the clinical improvement to refine cancer therapy and to identify biomarkers that would allow detection of patients at risk for the onset of malignancies in FPD/AML.

We collected DNA samples and clinical information of 73 individuals, belonging to 57 pedigrees, who have a history of familial thrombocytopenia and/or haematological malignancies, with the aim of identifying pedigrees with FPD/AML and uncovering recurrent mutations that drive the malignant transformation. Next-generation sequencing and single-cell sequencing strategy suggest that somatic mutation in *CDC25C* may be one of the early genetic events for leukaemic initiation in FPD/AML, and further stepwise acquisition of mutations such as *GATA2* leads to FPD/AML-associated leukaemic progression. These observations shed light on a part of leukemogenesis in FPD/AML.

Results

A novel gene target in haematological disorders. Thirteen patients in 7 pedigrees were diagnosed as having FPD/AML after screening for germline *RUNX1* mutations in 73 index patients; 7 of the 13 patients had developed haematological malignancies, while the other 6 only showed thrombocytopenia (Table 1). Most of the detected *RUNX1* mutations were point mutation in Runt homology domain or frame-shift mutation that lost transactivation domain, consistent with the previous reports[2,4]. As haploinsufficiency of *RUNX1* might cause familial thrombocytopenia with propensity to develop AML[1], we also examined whether the pedigrees have *RUNX1* loss of heterozygosity (LOH) or not. A synchronized quantitative-PCR method[6] and single-nucleotide polymorphism (SNP) sequencing detected no case with LOH in *RUNX1* in our cohort (Supplementary Fig. 1 and detailed in Methods). To systematically identify additional genetic alterations, we utilized whole-exome sequencing for two individuals from the same FPD/AML pedigree who shared a common *RUNX1*_p.Phe303fs mutation and who had developed MDS (subject 20) or myelofibrosis (subject 21) at the age of 37 and 17 years, respectively. In both these patients, the disease had progressed to AML[7]. Validation by Sanger sequencing and/or targeted deep sequencing of candidate mutations in paired tumour/normal DNA samples confirmed 10 (subject 20) and 8 (subject 21) somatically acquired nonsynonymous mutations (Table 2; Supplementary Figs 2–4; Supplementary Methods). Surprisingly, both patients carried the identical somatic *CDC25C* mutation (p.Asp234Gly), which had not been reported previously in human cancers (Fig. 1a,b). Prompted by this finding, we investigated *CDC25C* mutations in other FPD/AML cases by deep sequencing. In total, four of seven affected patients with haematological malignancies had *CDC25C* mutations, of which three carried the same p.Asp234Gly mutation. Moreover, *CDC25C* mutations were detected in an additional three FPD/AML patients who had not yet developed haematological malignancies, although the variant allele fractions (VAFs) were much lower in this group of patients than in those who had already developed haematological malignancies (Fig. 1c; Table 1). Thus, 7 of the 13 FPD/AML patients (53%) harboured a *CDC25C* mutation. *CDC25C* was also screened for mutations in 90 sporadic MDS and 53 AML patients, including 13 MDS and 3 AML cases who carried *RUNX1* mutations. No *CDC25C* mutations were identified in the 90 sporadic cases, except for the p.Ala344Val in an MDS patient bearing a *RUNX1* mutation, indicating that *CDC25C* mutations were significantly associated with germline, but not with somatic *RUNX1* mutations ($P = 0.004$; Supplementary Fig. 5; Supplementary Table 1).

Clonal evolution of FPD/AML. Deep sequencing of individual mutations that had been detected by whole-exome sequencing

Table 1 | Mutational status of *CDC25C* in FPD/AML patients.

Pedigree number	Subject number	RUNX1 mutation	Disease status	Age, years*	CDC25C mutation	VAF (%)
18	20	p.Phe303fs	MDS/AML	37/38	p.Asp234Gly	31.7/45.8
	21		MF/AML	17/18	p.Asp234Gly	31.1/39.0
19	22	p.Arg174*	AML	41	p.His437Asn	39.7
54	65	p.Ser140Asn	MDS	25	—	—
	66		AML	56	p.Asp234Gly	24.2
32	38	p.Leu445Pro	HCL	72	—	—
16	18	p.Thr233fs	Thrombocytopenia	—	p.Asp234Gly	5.9
53	62	p.Gly262fs	MDS	12	—	—
	63		Thrombocytopenia	—	—	—
	67		Thrombocytopenia	—	—	—
57	71	p.Gly172Glu	Pancytopenia†	—	p.Asp234Gly	8.3
	72		Thrombocytopenia	—	—	—
	73		Thrombocytopenia	—	p.Lys233Glu	1.8

AML, acute myeloid leukemia; FPD, familial platelet disorder; HCL, hairy cell leukemia; MDS, myelodysplastic syndrome; MF, myelofibrosis; VAF, variant allele fraction.
*Age at the time of diagnosis of each haematological malignancy is shown.
†Thrombocytopenia, leukopenia and iron-deficiency anemia were diagnosed.

Table 2 | Validated somatic mutations.

Gene symbol	Ref seq_no.	Amino-acid change	Position (hg19)	Base change	Mutation type	SIFT prediction	VAF at MDS/MF (%)	VAF at AML (%)
Subject 20								
AGAP4	NM_133446	p.Arg484Cys	g.chr10:46321905	C->T	Missense	Damaging	13.2	11.5
CDC25C	NM_001790	p.Asp234Gly	g.chr5:137627720	A->G	Missense	Damaging	31.7	45.8
CHEK2	NM_007194	p.Arg406His	g.chr22:29091740	G->A	Missense	Tolerated	14.6	11.1
COL9A1	NM_001851	p.Gly878Val	g.chr6:70926733	G->T	Missense	Damaging	9.6	26.4
DTX2	NM_001102594	p.Pro74Arg	g.chr7:76110047	C->G	Missense	Damaging	18.3	11.2
FAM22G	NM_001170741	p.Ser508Thr	g.chr9:99700727	T->A	Missense	Tolerated	10.2	27.6
GATA2	NM_001145661	p.Leu321His	g.chr3:128202758	T->A	Missense	Damaging	0.0	28.1
LPP	NM_001167671	p.Val538Met	g.chr3:188590453	G->A	Missense	Damaging	9.7	28.8
RP1L1	NM_178857	p.Ser215fs	g.chr8:10480295	insC	Frameshift	Damaging	14.2	12.7
SIGLEC9	NM_014441	p.Ser437Gly	g.chr19:51633253	A->G	Missense	Tolerated	27.4	42.5
Subject 21								
ANXA8L1	NM_001098845	p.Val281Ala	g.chr10:48268018	T->C	Missense	Damaging	30.8	36.8
CDC25C	NM_001790	p.Asp234Gly	g.chr5:137627720	A->G	Missense	Damaging	31.1	39.1
DENND5A	NM_001243254	p.Arg320Ser	g.chr11:9215218	A->C	Missense	Damaging	29.5	37.3
FER	NM_005246	p.Tyr634Cys	g.chr5:108382876	A->G	Missense	Damaging	1.4	30.4
FNDC1	NM_032532	p.Arg189Cys	g.chr6:159636081	C->T	Missense	Damaging	29.3	35.9
OR8U1	NM_001005204	p.Asn175Ile	g.chr11:56143623	A->T	Missense	Damaging	30.0	34.1
PIDD	NM_145886	p.Arg342Cys	g.chr11:802347	C->T	Missense	Damaging	3.3	28.3
ZNF614	NM_025040	p.Glu202Gly	g.chr19:52520246	A->G	Missense	Damaging	28.7	33.7

AML, acute myeloid leukemia; MDS, myelodysplastic syndrome; MF, myelofibrosis; SIFT, sorting intolerant from tolerant; VAF, variant allele fraction.

allowed accurate determination of their VAFs; on this basis, we could establish an inferred model of clonal evolution in terms of individual mutations in subjects 20 and 21 (Fig. 2a,b; Supplementary Fig. 6a,b). Intratumoral heterogeneity was evident at both MDS and AML phases in subject 20. According to the predicted model, a founding clone with a *CDC25C* mutation acquired additional mutations in *COL9A1*, *FAM22G* and *LPP* (group A), followed by the emergence of a *GATA2* mutation (group B), which was associated with leukaemic transformation, whereas the size of another subclone, defined by mutations in *CHEK2* and three other genes (group C), was unchanged. To validate this hierarchical model, single-cell genomic sequencing was performed using genomic DNA of 63 bone marrow cells from subject 20 when the patient was in the AML phase. Assuming that all cells harbour the *RUNX1* mutation, the false-negative rate of the procedure reached 35%, possibly due to biased allele amplification (Online Methods). However, this technique successfully demonstrated that the group A/B and group C mutations were mutually exclusive (Fig. 2c; Supplementary Table 2). To statistically evaluate this possibility, we assumed two hypotheses (H_0: the mutational status of genes in group A/B and group C is independent; H_1: mutations in group A/B and group C are mutually exclusive) and calculated each probability distribution (P_i: probability that the current results as shown in Fig. 2c were obtained under the hypothesis H_i). Our mutational profile data were achieved with a much higher likelihood under H_1 than H_0 (Supplementary Fig. 7 and detailed in Supplementary Methods). Similarly, the clonal architecture for subject 21 was portrayed in Fig. 2b and Supplementary Fig. 6b. In both scenarios, *CDC25C* mutations seemed to represent a founding mutation with the highest VAF, suggesting that the *CDC25C* mutation contributed to the establishment of a founding tumour population as an early genetic event, whereas progression to AML seemed to be accompanied by the appearance of additional mutations, indicating a multistep process in leukemogenesis.

Along with the somatic mutations found in subjects 20 and 21, a *GATA2* mutation was also identified in subject 22 (Fig. 3a). This patient developed AML with multilineage dysplasia, which led to the diagnosis of AML – MRC (myelodysplasia-related changes). Remission-induction therapies were only partially effective and the blast cell count was reduced from 54 to 5.6%, while dysplastic features persisted (Fig. 3b; Supplementary Fig. 8). Allogeneic stem cell transplantation was successfully performed from a human leukocyte antigen-matched unrelated donor and durable complete remission, with 100% donor chimerism, was achieved. During treatment, the VAF of the *GATA2* mutation decreased virtually in parallel with the blast cell percentage, while the VAF of the *CDC25C* mutation hovered at a high level before transplantation. Thus, we hypothesized that the *GATA2* mutation induced leukaemia progression in this patient, whereas the *CDC25C* mutation was associated with the pre-leukaemic status. Another *GATA2* mutation (p.Leu359Val) was found in subject 18, with a VAF (0.94%), who showed only thrombocytopenia without any signs of leukaemia progression and who had a small subclone with a concurrent *CDC25C* mutation (Fig. 3c). Although *GATA2* mutations are detected in a small number of patients with FPD/AML, the findings described above suggest that mutation of *GATA2* is a key factor promoting disease progression in FPD/AML (Fig. 3d).

Biological consequences of *CDC25C* mutations. We next investigated the possible impact of *CDC25C* mutation on clonal selection and evolution. CDC25C is a phosphatase that prevents premature mitosis in response to DNA damage at the G2/M checkpoint, while it is constitutively phosphorylated at Ser216 throughout interphase by c-TAK1 (refs 8–10). When phosphorylated at Ser216, CDC25C binds to 14-3-3 protein[11], leading to sequestration of CDC25C to the cytoplasm and its inactivation. Ba/F3 cells were transduced with retroviruses encoding the wild-type or mutant CDC25C containing each of the individual mutations (p.Asp234Gly, p.Ala344Val, p.His437Asn and p.Ser216Ala), and assayed for the phosphorylation status, 14-3-3 protein-binding capacity and intracellular localization of each of these proteins. The Ser216Ala mutant form

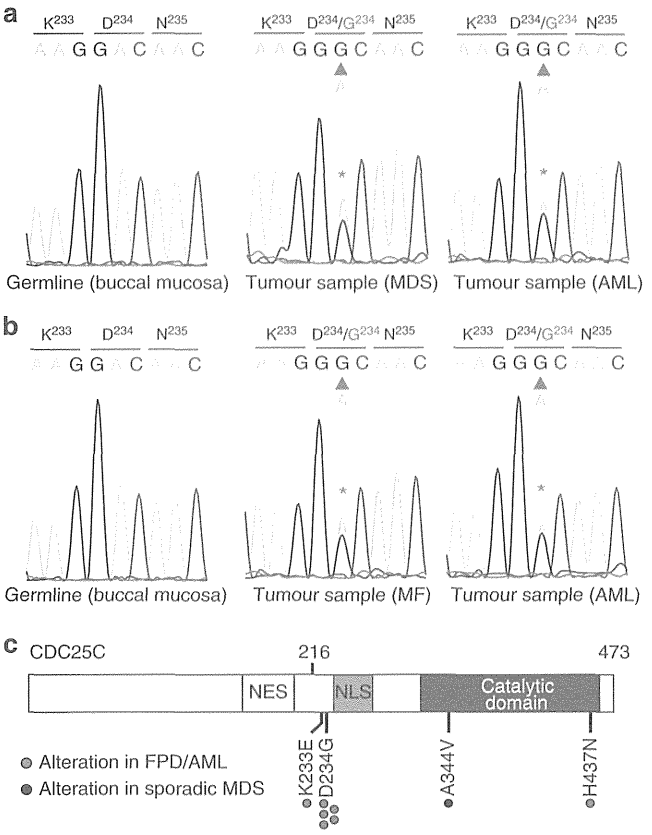

Figure 1 | Mutation in *CDC25C* recurs in cases of FPD/AML. (**a**,**b**) Sanger sequencing of *CDC25C* mutations found in whole-exome sequencing is shown. Both forward and reverse traces were available for each mutation, but only one trace is shown above. The results of buccal mucosa, pre-leukaemic phase and leukaemic phase is demonstrated for subject 20 (**a**) and subject 21 (**b**), respectively. (**c**) The distribution of alterations is shown for the CDC25C protein. NES, a putative nuclear export signal domain between amino acids 177–200; NLS, a putative nuclear localization sequence domain consisting of amino acids 240–244.

of CDC25C, which lacks the phosphorylation site, was used as a negative control. In all of the mutated forms of CDC25C, the capacity for binding to c-TAK1 was reduced (Fig. 4a,b; Supplementary Fig. 9a,b), resulting in decreased phosphorylation of CDC25C at Ser216 (Fig. 4c). Consequently, the mutant proteins failed to bind 14-3-3 protein efficiently (Fig. 4d,e; Supplementary Fig. 8c,d) and remained in the nucleus even during interphase (Fig. 4f; Supplementary Figs 10 and 11). In accordance with these observations, CDC25C mutants enhanced mitotic entry, which was exaggerated by low-dose radiation-induced DNA damage (Fig. 4g,h; Supplementary Fig. 12; Supplementary Methods). These results suggest that mutation of *CDC25C* results in disruption of the DNA checkpoint machinery. Next, we investigated why mutation of *CDC25C* is a frequent genetic event in FPD/AML. It is known that *RUNX1* mutations suppress DNA damage repair and subsequent cell cycle arrest in hematopoietic cells by means of transcriptional suppression of several genes that are involved in DNA repair[12,13]. We confirmed that FPD/AML-associated *RUNX1* mutations have similar effects, as we observed activation of the G2/M checkpoint mechanism in the presence of *RUNX1* mutations (Fig. 4i; Supplementary Fig. 13a,b). We found, however, that introduction of mutations in *CDC25C* resulted in enhanced mitosis entry, despite co-existence of *RUNX1* mutations (Fig. 4i). Therefore, we speculated that compromised DNA damage checkpoint mechanisms caused by mutations in *CDC25C* may contribute to malignant transformation, in concert with increased genomic instability due to *RUNX1* mutations.

Discussion

Whole-exome sequencing, followed by targeted deep sequencing, identified novel aspects of the pathogenesis of malignant transformation in FPD/AML. First, the high frequency of *CDC25C* mutations in FPD/AML underscores their major role in the development of haematological malignancies in FPD/AML patients. To our knowledge, *CDC25C* mutations have not been reported previously and represent a new recurrent mutational target in haematological malignancies, although *CDC25C* mutations have been reported in some solid carcinomas with unknown significance[14,15]. Furthermore, our functional assays support their biological significance, which is characterized by cell cycle progression and premature mitotic entry. Although the 5q31 minimally deleted region, in which CDC25C is located, is frequently detected in MDS, it seems to be associated with other oncogenic mechanisms since our functional assays suggested that *CDC25C* mutations in FPD/AML were gain-of-function type mutations that facilitate the mitotic entry by aberrant accumulation in the nucleus. Impaired DNA repair function mediated by germline *RUNX1* mutation may play a role in the generation of *CDC25C* mutations.

Evaluation of the allelic burden of mutated genes demonstrated that *CDC25* mutations are found with high VAFs in FPD/AML-derived leukaemia and with low VAFs in cases of thrombocytopenia. Our hierarchical model and clonal selection highlighted that mutation of *CDC25C* defines an initial event during malignant transformation and predates subclonal mutations in *GATA2* and other genes. On the basis of the observation that four of the seven FPD/AML patients with *CDC25C* mutations have developed leukaemia and that *CDC25C* mutations were actually detected in the leukaemic subclones, we speculated that a FPD/AML patient with a *CDC25C* mutation, but without clinically evident leukaemia, is at high risk for the onset of leukaemic progression. Examination of the allelic burden of *CDC25C* mutation may thus serve to evaluate the risk of leukaemic progression in patients with FPD/AML.

Among the mutations found in FPD/AML, mutations in *GATA2* were identified in 3 of 13 individuals (subjects 18, 20 and 22). *GATA2* mutations were frequently identified in FPD/AML-derived leukaemia (2/7) and in a patient with thrombocytopenia who had a small subclone bearing a *CDC25C* mutation (1/6). Although reports on the clinical relevance of *GATA2* mutations in myeloid malignancy are limited, several lines of evidence in this respect have recently been reported. *GATA2* mutations are frequently found in a subgroup of patients with cytogenetically normal AML with biallelic *CEBPA* gene mutations[16], which account for ~4% of AML. Germline *GATA2* mutations are also observed in disorders linked to an increased propensity for the development of MDS and AML, including Emberger syndrome, MonoMAC syndrome and dendritic cells, monocytes, B and natural killer cells deficiency[17–20]. The alterations in *GATA2* (leading to p.Leu321His and p.Leu359Val), which were found in FPD/AML patients in this study, are located in the part of the gene encoding the N-terminal and C-terminal zinc-finger domains, respectively (Fig. 3d). Mutations affecting the identical amino acids have been reported in AML patients bearing *CEBPA* mutations and chronic myeloid leukaemia patients in blast crisis[16,21]. Thus, *GATA2* mutation may contribute to AML progression in collaboration with *RUNX1* and/or *CDC25C* mutations. Furthermore, although

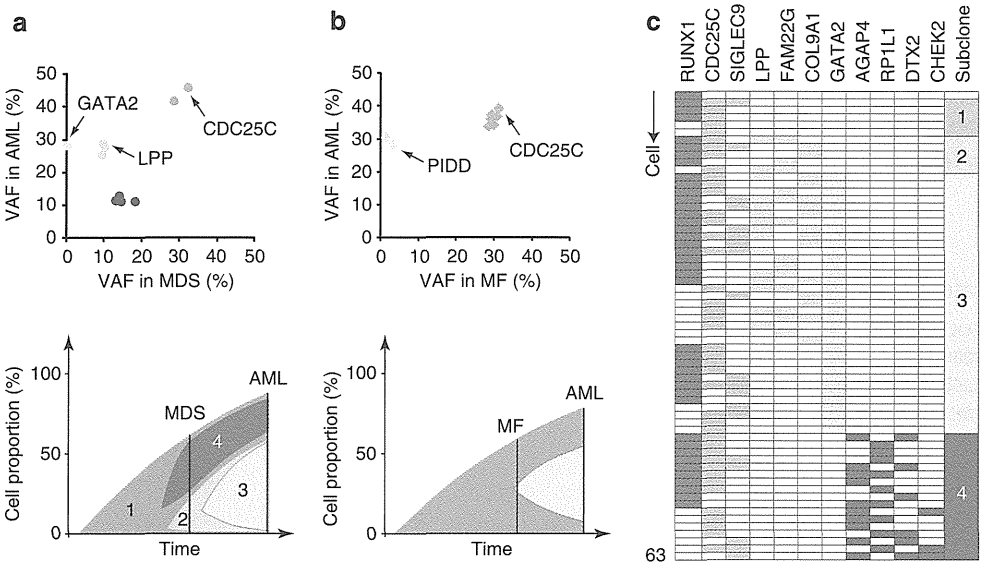

Figure 2 | Clonal evolution of FPD/AML-related myeloid disorders. (**a**,**b**) Observed variant allele fraction (VAF) of validated mutations are listed in Table 2, in both pre-leukaemic and leukaemic phases, are shown in diagonal plots (top) for subject 20 (**a**) and subject 21 (**b**). Predicted chronological behaviours in different leukemia subclones are depicted below each diagonal plot. Distinct mutation clusters are displayed by colour. The vertical axis represents cell proportion of each clone calculated by VAF × 2 (%) (because all the mutations were heterozygous), regarding the whole bone marrow as 100%. (**c**) Mutation status of each bone marrow cell from subject 20 during the acute myeloid leukemia (AML) phase. The vertical axis represents each cell ($n = 63$) and the horizontal axis displays each gene mutation. Coloured columns show that the corresponding cell harbours gene mutation(s) as defined in Online Methods. Subclone numbers shown in the right row correspond to the numbers in the lower figure of **a**.

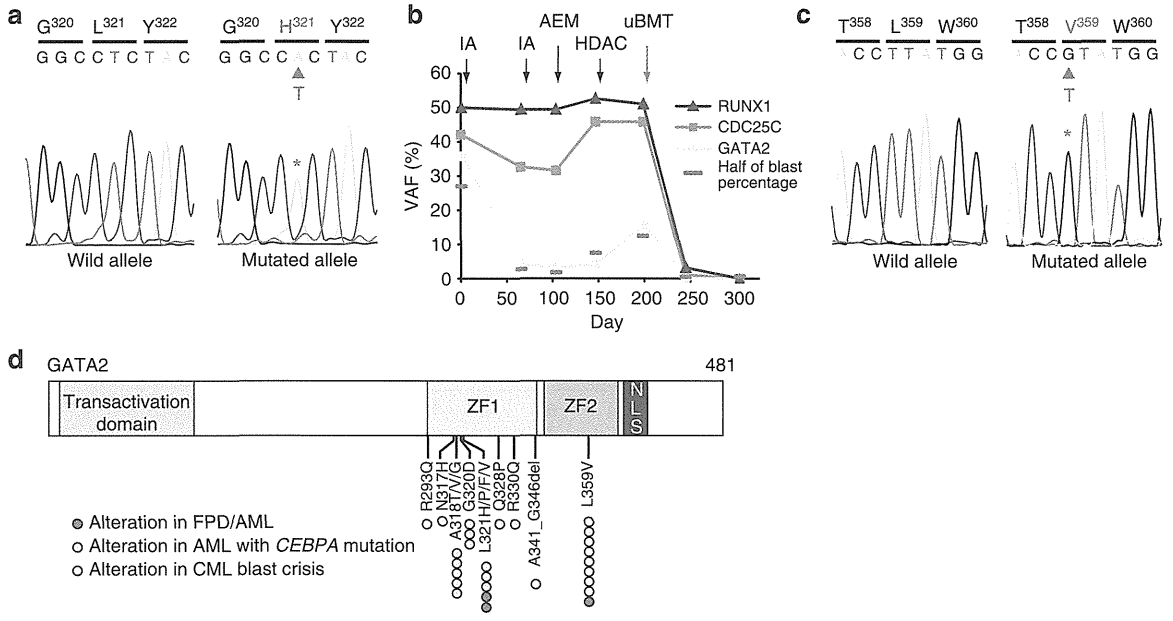

Figure 3 | *GATA2* mutations in FPD/AML. The result of Sanger sequencing for *GATA2* p.Leu321His mutation in subject 22 (**a**) and Leu359Val mutation in subject 18 (**c**) validated with subcloning strategy by methods shown in Supplementary Methods. (**b**) Variant allele fractions (VAFs) of *RUNX1*, *CDC25C* and *GATA2* mutation in subject 22 are demonstrated with the time course of treatment. Half the value of the blast cell percentage, which corresponds to the allele frequency of a heterozygous mutation, is also shown by a red bar. IA, idarubicine + Ara-C; AEM, Ara-C + etoposide + mitoxantrone; HDAC, high-dose Ara-C; uBMT, unrelated bone marrow transplantation. (**d**) Schematic representation of *GATA2* mutations. *GATA2* mutations that were identified in FPD/AML are displayed together with mutations found in AML with *CEBPA* mutation[16] as well as in CML patients in blast crisis[21]. ZF, zinc-finger domain; NLS, a putative nuclear localization sequence domain.

another report identified somatic *CBL* mutation with acquired 11q uniparental disomy as a second hit as being responsible for leukaemic transformation in FPD/AML[22], *CBL* mutations were not detected in our series of FPD/AML samples.

Although the precise pathogenetic roles of *CDC25C* mutations remain unclear, we presume that mutant CDC25C alleles confer a proliferative advantage under certain circumstances in which DNA repair machinery is compromised, such as that mediated by

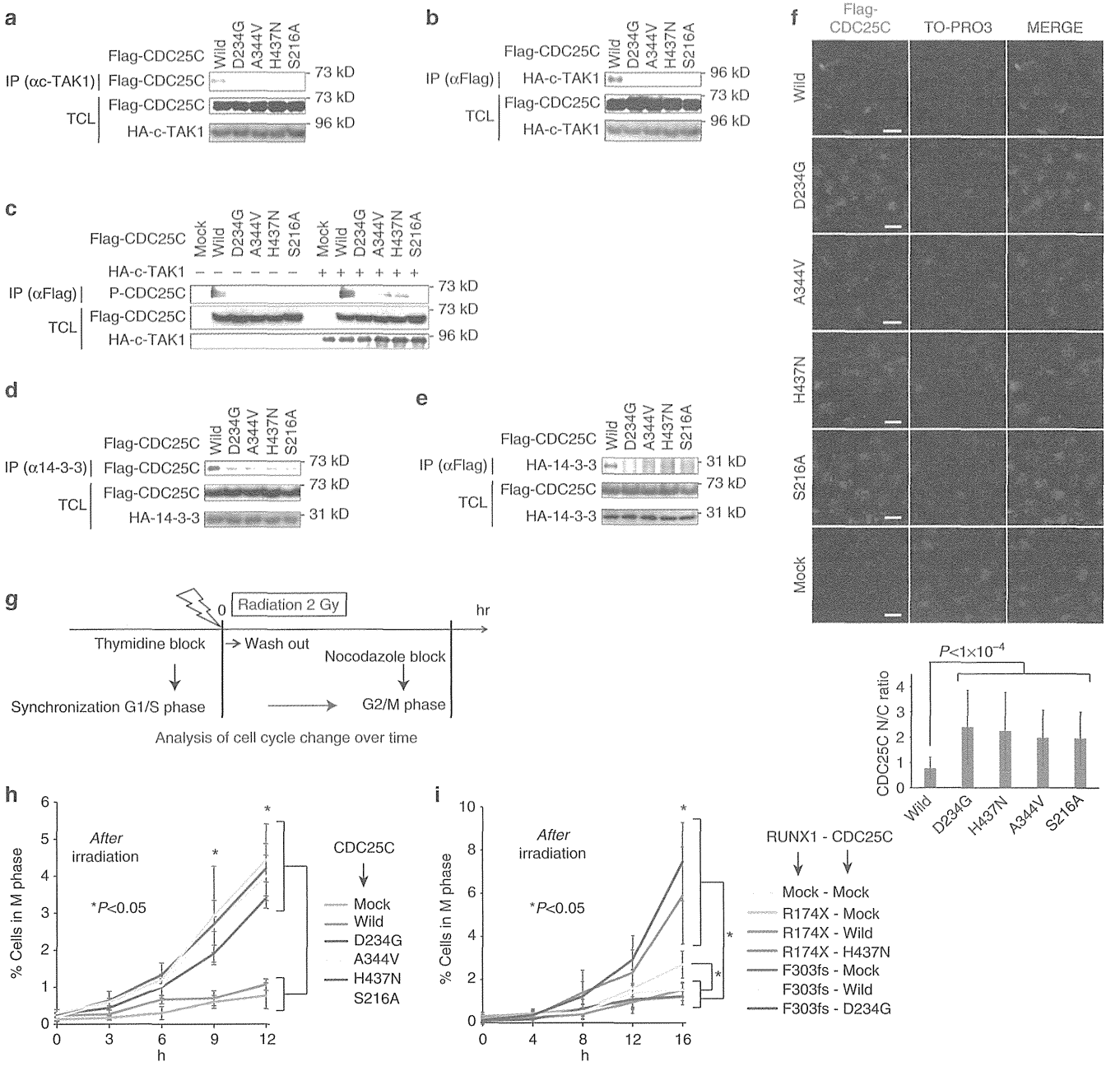

Figure 4 | Mutated CDC25C enhances mitotic entry. (**a**) HEK293T cells were transiently transfected with constructs encoding Flag-tagged CDC25C wild type or mutants, as indicated, and cell lysates were immunoprecipitated with anti-c-TAK1 antibody. Binding capacity of CDC25C was evaluated by western blotting. IP, immunoprecipitation; TCL, total cell lysate. (**b**) Reciprocal immunoprecipitation of **a** using anti-Flag (CDC25C) antibody for immunoprecipitation. (**c**) Left half; cell lysates were immunoprecipitated with anti-Flag antibody. Phosphorylation levels of CDC25C were assessed by phosphorylated-Ser216-specific anti-CDC25C antibody. Right half; the same experiment was performed with cell lysates from HEK293T cells transfected with constructs encoding Flag-tagged CDC25C wild type or mutants and HA-tagged c-TAK1. (**d**) Mutated CDC25C showed reduced capacity for binding to 14-3-3. Cell lysates were immunoprecipitated with anti-14-3-3 antibody and binding capacity of CDC25C was evaluated. (**e**) Reciprocal immunoprecipitation of **d** using anti-Flag (CDC25C) antibody for immunoprecipitation. (**f**) Localization of CDC25C or its mutants was visualized by immunofluorescence. Anti-Flag antibody and Alexa Fluor 555 antibody was used for visualization of CDC25C. N/C ratio of each cell was calculated as detailed in Supplementary Methods and Supplementary Fig. 10. The mean and s.d. of the N/C ratio is presented. Statistical significance of difference was determined by unpaired Student's *t*-test ($n>30$ for each). Scale bar, 10 μm. (**g**) Schematic description of the method used for evaluation of mitotic entry. (**h**) Mitotic entry of CDC25C-mutated cells. Percentage of mutated CDC25C-transduced cells in the M phase was compared with that of wild-type CDC25C-transduced cells. *P* values were calculated using Student's *t*-test and the differences between groups, as indicated, were all statistically significant ($^*P<0.05$) at 10 and 12 h after irradiation ($n=3$). The average and s.d. is presented. (**i**) Mutated RUNX1 and CDC25C were co-expressed in Ba/F3 cells, as indicated, and mitosis entry of these cells was evaluated. The differences between groups, as indicated, were all statistically significant ($^*P<0.05$ at 16 h after washout of thymidine ($n=3$). *P* values were determined using the Student's *t*-test. The average and s.d. is presented.

a germline *RUNX1* mutation. In addition, as Turowski and colleagues reported that CDC25C was involved in S phase entry in addition to mitotic entry[23], release from thymidine-induced G1/S block may be affected by some unknown machinery mediated by mutated CDC25Cs, which might affect the results when we observed G2/M phase fraction of these cells. It is not clear why *CDC25C* mutations are repetitively documented in FPD/AML, but not in sporadic MDS or AML cases. One possibility is that in the presence of a *RUNX1* mutation, as an initial event, an extended period is required before an additional *CDC25C* mutation is acquired. This proposal is supported by the clinical observation that ~40% of patients with FPD/AML develop leukaemia in their 30s[5]; however, the mutational status in *CDC25C* in the reported cohort was unknown.

One of the important problems in the research of FPD/AML is that definitive diagnostic criteria have not been established yet. For this purpose, more extensive studies are required for accumulating clinical characterization, genetic information and functional examination as to whether a *RUNX1* variant in families with thrombocytopenia and/or haematological malignancy is causal[24]. We clarified tentative diagnostic criteria for FPD/AML, which was used in this study (in Methods). Regarding the three missense variants in our study (p.Ser140Asn in pedigree 54, p.Gly172Glu in pedigree 57 and p.Leu445Pro in pedigree 32), Ser140 and Gly172 have been reported to be mutated in sporadic AML and/or MDS cases[25,26]. In addition, induced pluripotent stem cells from a FPD/AML pedigree with p.Gly172Glu recapitulate the phenotype of FPD/AML after hematopoietic differentiation[27]. Ser140 has been also shown to be important for RUNX1 conformation, and a mutation of this site affects hydrogen bonds and results in functional loss[28,29]. Furthermore, all the three missense variants have not been reported in the following SNP database: SNP database (dbSNP) (http://www.ncbi.nlm.nih.gov/projects/SNP), the 1000 Genomes Project (http://www.1000genomes.org), HGVB (http://www.genome.med.kyoto-u.ac.jp/SnpDB/index.html). They were also predicted as 'damaging' by Polyphen-2 (http://genetics.bwh.harvard.edu/pph2/), SIFT (http://sift.jcvi.org/) and PROVEAN (http://provean.jcvi.org/index.php). Therefore, we regarded the pedigrees with these *RUNX1* variants as having FPD/AML in this study. However, regarding pedigree 32 with p.Leu445Pro, we could not completely exclude the possibility of incidental co-occurrence of a possible non-causal *RUNX1* germline variant and hairy cell leukaemia, although co-occurrence of them is supposed to be rare. In addition, we should bear in mind the somatic as well as germline LOH of *RUNX1*, which contributes to thrombocytopenia and/or leukemogenesis in FPD/AML.

In conclusion, our results indicate that FPD/AML-associated leukaemic transformation is due to stepwise acquisition of mutations and clonal selection, which is initiated by a *CDC25C* mutation in the pre-leukaemic phase, and is further driven by mutations in other genes including *GATA2* (Supplementary Fig. 14). The identification of *CDC25C* as the target gene responsible for the leukaemic transformation will facilitate diagnosis and monitoring of individuals with FPD/AML, who are at an increased risk of developing life-threatening haematological malignancy.

Methods

Subjects. Studies involving human subjects were done in accordance with the ethical guidelines for biomedical research involving human subjects, which was developed by the Ministry of Health, Labour and Welfare, Japan; the Ministry of Education, Culture, Sports, Science, and Technology, Japan; and the Ministry of Economy, Trade, and Industry, Japan, and enforced on 29 March 2001. This study was approved by ethical committee of the University of Tokyo and each participating institution. Written informed consent was obtained from all patients whose samples were collected after the guideline was enforced. All animal experiments were approved by the University of Tokyo Ethics Committee for Animal Experiments. The clinical data, peripheral blood sample and buccal mucosa of the patients whose pedigree contained two or more individuals with thrombocytopenia and/or any haematological malignancies were collected from participating institutions. Platelet threshold depended on each institution's judge and any haematological malignancies were allowed. The diagnoses were self-reported. When all the following four criteria were fulfilled, the patient was considered as having FPD/AML in this study: (1) the pedigree has two or more individuals with thrombocytopenia and/or any haematological malignancies; (2) a germline *RUNX1* variant, including missense, nonsense, frameshift, insertion and deletion, is confirmed by Sanger sequencing and a synchronized quantitative-PCR method in at least one family member; (3) the *RUNX1* variant has not been reported in public dbSNP; (4) no germline mutations were detected in the following 16 genes: *GATA2*, *GATA1*, *CEBPA*, *MPL*, *MYH9*, *MYL9*, *GP1BA*, *GP9*, *MASTL*, *HOXA11*, *CBL*, *DIDO1*, *TERT*, *ANKRD26*, *GFI1B* and *SRP72*. Regarding the last criterion, 16 genes were selected because they have been reported to be responsible for familial thrombocytopenia and/or haematological malignancies.

Whole-exome sequencing. Genomic DNA was extracted from samples using the QIAamp DNA Mini kit (Qiagen). Exome capture was performed. Enriched exome fragments were subjected to sequencing using HiSeq2000 (Illumina). We removed any potential somatic mutations that were observed in dbSNP (http://www.ncbi.nlm.nih.gov/projects/SNP) or in the 1000 Genomes Project (http://www.1000genomes.org) data. All candidate single-nucleotide variations and indels, which were predicted to be deleterious by the Polyphen-2 algorithm, were validated by deep sequencing and Sanger sequencing. Genomic DNA samples from the buccal mucosa of the two patients (subject 20 and subject 21) were used as references. All candidate somatic mutations were validated by Sanger sequence and deep sequencing using primers listed in Supplementary Tables 3 and 4.

Deep sequencing. Using genomic DNA of the patients as template, each targeted region was PCR amplified with specific primers (Supplementary Table 4). The amplification products from an individual sample were combined and purified with the AMpure XP Kit (Beckman Coulter) and library preparation was carried out using the Ion Xpress Fragment Library Kit (Life Technologies) according to the manufacturer's instructions. The Agilent 2100 Bioanalyzer (Agilent Technologies) and the associated High Sensitivity DNA kit (Agilent Technologies) were used to determine quality and concentration of the libraries. The amount of the library required for template preparation was calculated using the template dilution factor calculation described in the protocol. Emulsion PCR and enrichment steps were carried out using the Ion OneTouch 200 Template Kit v2 DL (Life Technologies). Sequencing was undertaken using Ion Torrent PGM and Ion 318 chips Kit v2 (Life Technologies). The Ion PGM 200 Sequencing Kit (Life Technologies) was used for sequencing reactions, following the recommended protocol. The presence of *CDC25C* and *GATA2* mutations was also validated by a subclone strategy for DNA sequence analysis.

Single-cell sequencing and genome amplification. Single cells were separated from the bone marrow of subject 20 at AML phase using FACSAria II (BD biosciences) (Supplementary Fig. 15a). Each cell was deposited into individual wells of a 96-well plate. Single cells were lysed and whole genome from single cell was amplified using GenomePlex Single Cell Whole-Genome Amplification Kit (Sigma-Aldrich). Mutation status of each gene was analysed by direct sequencing with specific primers (Supplementary Table 5). To improve the sensitivity of this procedure, we used multiple primer sets for detecting a single-nucleotide variation. We estimated the false-negative rate of this procedure based on the ratio of RUNX1 mutation, which is supposed to be observed in all of the cells. The false-negative rate was estimated to be 35% (22 cells out of 63 cells, Supplementary Table 2), which is consistent with the manufacturer's bulletin reporting the allelic dropout of 30%. In light of these results, we regard those cells with at least one gene mutation in a mutational group (coloured in red, orange, green, blue or purple) as being positive for gene mutations of the corresponding group. To assess whether mutations in *LPP*, *FAM22G*, *COL9A1* and *GATA2* and mutations in *AGAP4*, *RP1L1*, *DTX2* and *CHEK2* were mutually exclusive, we performed a statistical analysis as follows. First of all, we determine a matrix **A** that virtually represents the mutational status of eight genes (1: *LPP*, 2: *FAM22G*, 3: *COL9A1*, 4: *GATA2*, 5: *AGAP4*, 6: *RP1L1*, 7: *DTX2* and 8: *CHEK2*) of 57 cells. Concretely, **A** is defined as follows:

$$\mathbf{A}=\begin{pmatrix} a_{1,1} & \cdots & a_{8,1} \\ \vdots & \ddots & \vdots \\ a_{1,57} & \cdots & a_{8,57} \end{pmatrix} \quad a_{i,j}=\begin{cases} 0: \text{if gene i of cell j is wildtype} \\ 1: \text{if gene i of cell j is mutated} \end{cases} \qquad (1)$$

On the other hand, a matrix **R** indicates data from the actual experimental results of mutational analysis as shown in Fig. 2c. Elements of **R** is provided in

Supplementary Table 2.

$$\mathbf{R}=\begin{pmatrix} r_{1,1} & \cdots & r_{8,1} \\ \vdots & \ddots & \vdots \\ r_{1,57} & \cdots & r_{8,57} \end{pmatrix} \quad r_{i,j}=\begin{cases} 0: \text{if gene i of cell j is wild type} \\ 1: \text{if gene i of cell j is mutated} \\ 2: \text{if mutational status of gene i of cell j is undetermined} \end{cases} \tag{2}$$

Then we assumed two hypotheses: H_0 and H_1.

H_0: the mutational status of genes $1\sim4$ and genes $5\sim8$ is independent. Each matrix elements of A are randomly assigned 0 or 1 (at ratio of 1:1) independently of each other.

H_1: mutations in genes $1\sim4$ and genes $5\sim8$ are mutually exclusive, and cells $1\sim40$ harbour mutations of genes $1\sim4$, while cells $41\sim57$ harbour mutations of genes $5\sim8$. In mathematical representation,

$$a_{i,j}=\begin{cases} 0: (5\le i\le 8 \text{ and } 1\le j\le 40) \text{ and } (1\le i\le 4 \text{ and } 41\le j\le 57) \\ 0 \text{ or } 1 \text{ randomely}: (1\le i\le 4 \text{ and } 1\le j\le 40) \text{ and } (5\le i\le 8 \text{ and } 41\le j\le 57) \end{cases} \tag{3}$$

We assumed matrices A_0 and A_1 that represent virtually generated mutational status under the hypotheses H_0 and H_1, and calculate the probability of substantializing R for given A_0 and A_1.

$P_0(R/A_0)$ and $P_1(R/A_1)$ can be calculated for given matrices A_0 and A_1 under the condition as follows:

Probability that we cannot determine whether a cell has mutation in gene X when the cell does not actually have a mutation; 28% (based on our data shown in Supplementary Table 2).

Probability that we judge that a cell has a mutation in gene X when the cell does not actually have a mutation; 5% (because it is very unlikely to happen).

Probability that we can judge correctly that a cell does not have a mutation in gene X when the cell does not actually have a mutation; 67% ($100-28-5=67\%$).

Probability that we cannot determine whether a cell has mutation in gene X when the cell actually has a mutation; 28% (based on our data shown in Supplementary Table 2).

Probability that we judge that a cell has a mutation in gene X when the cell actually has a mutation; 35% (the estimated false-negative rate based on the ratio of *RUNX1* mutation).

Probability that we can judge correctly that a cell has a mutation in gene X when the cell actually has a mutation; 37% ($100-28-35=37\%$).

Put it simply, P_0 represents the probability that one can get the mutational profile R when a cell harbours mutations independently of each other, while P_1 indicates the probability that R is realized under the condition where mutations in gene groups $1\sim4$ and $5\sim8$ are exclusive. Because A_0 and A_1 that meet the hypotheses H_0 and H_1 can be generated innumerably, we conducted a computational simulation to acquire the distribution of P_0 and P_1 by generating A_0 and A_1 100,000 times. For visibility, horizontal axis is converted to $-\ln(P)$.

Synchronized quantitative-PCR. These experiments were performed mostly as described previously[6]. Briefly, genomic DNA was denatured 95 °C for 5 min and iced immediately. Using the LightCycler 480 Instrument II (Roche), thermal cycling was performed with denatured genomic DNA, forward and reverse primers (Supplementary Table 6), THUNDERBIRD SYBR qPCR mix (TOYOBO). Threshold cycle scores were determined as the average of triplicate samples. We designed 27 primers for *RUNX1* and 3 reproducible primers (that is, primer RUNX-9, RUNX-19 and RUNX-20) were chosen by preparatory experiments. RPL5-2 and PRS7-1 primers, which were authorized previously[6], were also utilized as controls. In addition, genomic DNA extracted from the bone marrow sample of a MDS patient with a chromosome 21 deletion was also examined with the same primers as a control of *RUNX1* locus copy-number loss. Crossing points (Cps) of designed primers were examined by quantitative PCR. *RUNX1* locus copy-number relative to RPL5-2 was calculated using Cps of RUNX-9 and RPL5-2, with RPL5-2 values set at 2. Similar results were obtained when Cps of RUNX-19, RUNX-20 or RPS7-1 values were used.

LOH detection with SNP sequencing. To examine the existence of uniparental disomy, we designed four specific primers to detect nine SNPs in *RUNX1*, which are frequently seen (>40%) (Supplementary Table 7). Direct sequencing was performed with the primers, and heterogeneity of SNPs was examined.

Chemicals and immunological reagents. Thymidine and nocodazole were purchased from Sigma-Aldrich. Anti-CDC25C, anti-phospho-CDC25C (Ser216) and anti-beta-actin antibodies were purchased from Cell Signaling Technology. Anti-HA monoclonal antibody was purchased from MBL. Rabbit anti-Flag monoclonal antibody was purchased from Sigma-Aldrich. Anti-HA was purchased from Roche. Mouse anti-phospho-histone H2AX (Ser139) antibody and Alexa Fluor 488 mouse anti-phospho-H3 (Ser10) antibody were purchased from Merck Millipore. Alexa Fluor 488 rabbit anti-mouse immunoglobulin (Ig)G, Alexa Fluor 488 goat anti-rabbit IgG and Alexa Fluor 555 goat anti-rabbit IgG were purchased from Invitrogen. TO-PRO3 was purchased from Molecular Probes. Rabbit anti-14-3-3 Sigma antibody was purchased from Bethyl laboratories. Sheep anti-c-TAK1 antibody was purchased from Exalpha Biologicals. Anti-sheep IgG-HRP was purchased from RSD. Nonviable cell exclusion was performed by 7-AAD Viability Staining Solution (BioLegend).

Subclone strategy and direct sequencing. Using genomic DNA of the patients as template, each targeted region was amplified by PCR with specific primers (Supplementary Table 4). PCR products were purified with illustra ExoStar (GE Healthcare) and subcloned into *Eco*RV site of pBluescript II KS(−) (Stratagene). Ligated plasmids were transformed into *E. coli* strain XL1-Blue by 45 s heat shock at 42 °C. Positive transformants were incubated on LB plates containing 100 μg ml^{-1} ampicillin supplemented with X-gal (Sigma-Aldrich) and isopropyl β-D-1-thiogalactopyranoside (Sigma-Aldrich). For colony PCR, a portion of a white colony was directly added to a PCR mixture as the DNA template. Insert region was amplified by PCR procedure with T3 and T7 universal primers, purified with illustra ExoStar (GE Healthcare Life Sciences), and sequenced by the Sanger method with T3 and T7 primers using BigDye Terminator v3.1 Cycle Sequencing kit (Applied Biosystems) and ABI Prism 310 Genetic Analyzer (Life Technologies).

Immunoprecipitation and western blotting. These experiments were performed as described previously[30]. Briefly, HEK293T cells were transiently transfected with mammalian expression plasmids encoding Flag-tagged CDC25C and its mutants, HA-tagged 14-3-3 or c-TAK1. All plasmids were sequence verified. After 48 h, cell lysates were collected and incubated with an antibody (anti-HA antibody (1:200, 3 h), anti-Flag antibody (1:200, 3 h), anti-c-TAK1 antibody (1:150, 3 h) and anti 14-3-3 antibody (1:150, 3 h)). After incubation, the cell lysates were incubated with protein G-Sepharose (GE Healthcare) for 1 h. The precipitates were stringently washed with high salt-containing wash buffer and analysed by western blotting. Anti-Flag (HRP-conjugated, Sigma-Aldrich), anti-HA (MBL), anti-HA (HRP-conjugated, Roche), anti-CDC25C (Cell Signaling Technology), anti-phospho-CDC25C (Ser216) (Cell Signaling Technology), anti-c-TAK1 antibody (Exalpha Biologicals) or anti-14-3-3 antibody (Bethyl laboratories) antibodies and Immunostar LD (Wako) was used for detection. Original gel images of western blot analysis are shown in Supplementary Fig. 16.

Cell cycle synchronization and analysis for mitosis entry. After transduction of wild-type CDC25C or its mutated forms to murine lymphoid cell line Ba/F3 cells (RIKEN BioResource Center), double-thymidine block was performed to obtain cell cycle synchronization at G1/S phase. In brief, 2 mM of thymidine was added to the medium. After 16 h, cells were washed and released from the first thymidine for 8 h. A second block was initiated by adding 2 mM of thymidine, and cells were maintained for 16 h. Then thymidine was washed out and the cells were incubated with 1 mM nocodazole with or without 2 Gy of irradiation (Supplementary Fig. 10a). Ba/F3 cells were fixed over time with 75% ethanol in phosphate-buffered saline (PBS) at 4 °C overnight and permeabilized with 2% Triton-X at 4 °C for 15 min. The cells were stained with anti-phospho-H3 (Ser10) Alexa Fluor 488 conjugated antibody (dilution, 1:200) in PBS with 2% fetal calf serum at 4 °C for 30 min and then treated with 5% propidium iodide and 1% RNase in PBS at room temperature (RT) for 30 min. Cell cycle was analysed using a BD LSR II Flow cytometer (BD biosciences) (Supplementary Fig. 15b). To assess the cooperation of *CDC25C* and *RUNX1* mutation, wild-type or mutant (D234G, H437N) pMXs-neo-Flag-CDC25C and mutant (F303fsX566, R174X) pGCDNsam-IRES-KusabiraOrange-Flag-RUNX1 were retrovirally transduced into Ba/F3 cells.

Immunofluorescent microscopic analysis. These experiments were performed as described previously[30]. Briefly, Ba/F3 cells were fixed, permeabilized and blocked. Staining for phosphorylated histone H2AX was performed with anti-phospho-histone H2AX (Ser139) antibody (dilution, 1:500; Merck Millipore) at RT for 3 h. After washing with PBS three times and with 1% bovine serum albumin in PBS, the cells were treated with Alexa Fluor 488 rabbit anti-mouse IgG (dilution, 1:500; Invitrogen) and TO-PRO3 (dilution, 1:1,000; Molecular Probes) for 1 h. The proteins were visualized using FV10i (Olympus) or BZ-9000 (Keyence). The percentage of γH2AX foci-positive cells was determined by examining 100 cells per sample. Three independent experiments were performed. To evaluate the localization of CDC25C, Ba/F3 cells were treated with 2 mM thymidine for 12 h and stained. Staining was underwent with anti-Flag antibody or anti-CDC25C antibody at RT for 3 h. After washing, the cells were treated with Alexa Fluor 488 or 555 antibody and TO-PRO3 for 1 h. The mean intensity of CDC25C in the nucleus and cytoplasm of each cell was measured within a region of interest placed within the nucleus and cytoplasm (Supplementary Fig. 10). Similarly, the background intensity was quantified within the region of interest placed outside the cells. All the measurements were performed using the Fluoview FV10i software or ImageJ. The background-subtracted intensity ratio of the nucleus to cytoplasm was calculated in >30 cells in each specimen.

Retrovirus production. The procedures were performed as described previously[30]. Briefly, Plat-E packaging cells were transiently transfected with each retroviral construct using the calcium phosphate precipitation method, and supernatant

containing retrovirus was collected 48 h after transfection and used for infection after it was centrifuged overnight at 10,000 r.p.m.

Statistical analysis. To compare data between groups, unpaired Student's *t*-test was used when equal variance were met by the *F*-test. When unequal variances were detected, the Welch *t*-test was used. Differences were considered statistically significant at a *P* value of <0.05.

References

1. Song, W. J. *et al.* Haploinsufficiency of CBFA2 causes familial thrombocytopenia with propensity to develop acute myelogenous leukaemia. *Nat. Genet.* **23,** 166–175 (1999).
2. Ichikawa, M. *et al.* A role for RUNX1 in hematopoiesis and myeloid leukemia. *Int. J. Hematol.* **97,** 726–734 (2013).
3. Cameron, E. R. & Neil, J. C. The Runx genes: lineage-specific oncogenes and tumor suppressors. *Oncogene* **23,** 4308–4314 (2004).
4. Nickels, E. M., Soodalter, J., Churpek, J. E. & Godley, L. A. Recognizing familial myeloid leukemia in adults. *Ther. Adv. Hematol.* **4,** 254–269 (2013).
5. Liew, E. & Owen, C. Familial myelodysplastic syndromes: a review of the literature. *Haematologica* **96,** 1536–1542 (2011).
6. Kuramitsu, M. *et al.* Extensive gene deletions in Japanese patients with diamond-blackfan anemia. *Blood* **119,** 2376–2384 (2012).
7. Kirito, K. *et al.* A novel RUNX1 mutation in familial platelet disorder with propensity to develop myeloid malignancies. *Haematologica* **93,** 155–156 (2008).
8. Boutros, R., Lobjois, V. & Ducommun, B. CDC25 phosphatases in cancer cells: key players? Good targets? *Nat. Rev. Cancer* **7,** 495–507 (2007).
9. Kastan, M. B. & Bartek, J. Cell-cycle checkpoints and cancer. *Nature* **432,** 316–323 (2004).
10. Peng, C. Y. *et al.* C-TAK1 protein kinase phosphorylates human Cdc25C on serine 216 and promotes 14-3-3 protein binding. *Cell Growth Differ.* **9,** 197–208 (1998).
11. Lopez-girona, A., Furnari, B., Mondesert, O. & Early, P. R. Nuclear localization of Cdc25 is regulated by DNA damage and a 14-3-3 protein. *Nature* **397,** 172–175 (1999).
12. Satoh, Y., Matsumura, I., Tanaka, H. & Harada, H. C-terminal mutation of RUNX1 attenuates the DNA-damage repair response in hematopoietic stem cells. *Leukemia* **26,** 303–311 (2011).
13. Krejci, O. *et al.* p53 signaling in response to increased DNA damage sensitizes AML1-ETO cells to stress-induced death. *Blood* **111,** 2190–2199 (2008).
14. Park, J. *et al.* Mutation profiling of mismatch repair-deficient colorectal cancers using an in silico genome scan to identify coding microsatellites advances in brief mutation profiling of mismatch repair-deficient colorectal cancers using an in silico genome scan to Ide. *Cancer Res.* **62,** 1284–1288 (2002).
15. Vassileva, V., Millar, A., Briollais, L., Chapman, W. & Bapat, B. Genes involved in DNA repair are mutational targets in endometrial cancers with microsatellite instability. *Cancer Res.* **62,** 4095–4099 (2002).
16. Greif, P. A. *et al.* GATA2 zinc finger 1 mutations associated with biallelic CEBPA mutations define a unique genetic entity of acute myeloid leukemia. *Blood* **120,** 395–403 (2012).
17. Ostergaard, P. *et al.* Mutations in GATA2 cause primary lymphedema associated with a predisposition to acute myeloid leukemia (Emberger syndrome). *Nat. Genet.* **43,** 929–931 (2011).
18. Hahn, C. N. *et al.* Heritable GATA2 mutations associated with familial myelodysplastic syndrome and acute myeloid leukemia. *Nat Genet.* **43,** 1012–1017 (2011).
19. Hsu, A. P. *et al.* Mutations in GATA2 are associated with the autosomal dominant and sporadic monocytopenia and mycobacterial infection (MonoMAC) syndrome. *Blood* **118,** 2653–2655 (2011).
20. Dickinson, R. E. *et al.* Exome sequencing identifies GATA-2 mutation as the cause of dendritic cell, monocyte, B and NK lymphoid deficiency. *Blood* **118,** 2656–2658 (2011).
21. Zhang, S.-J. *et al.* Gain-of-function mutation of GATA-2 in acute myeloid transformation of chronic myeloid leukemia. *Proc. Natl Acad. Sci. USA* **105,** 2076–2081 (2008).
22. Hasegawa, D. *et al.* CBL mutation in chronic myelomonocytic leukemia secondary to familial platelet disorder with propensity to develop acute myeloid leukemia (FPD/AML). *Blood* **119,** 2612–2614 (2012).
23. Turowski, P. *et al.* Functional cdc25C dual-specificity phosphatase is required for S-phase entry in human cells. *Mol. Biol. Cell* **14,** 2984–2998 (2003).
24. Michaud, J. *et al.* In vitro analyses of known and novel RUNX1/AML1 mutations in dominant familial platelet disorder with predisposition to acute myelogenous leukemia: Implications for mechanisms of pathogenesis. *Blood* **99,** 1364–1372 (2002).
25. Kohlmann, A. *et al.* Monitoring of residual disease by next-generation deep-sequencing of RUNX1 mutations can identify acute myeloid leukemia patients with resistant disease. *Leukemia* **28,** 129–137 (2014).
26. Chen, C. Y. *et al.* RUNX1 gene mutation in primary myelodysplastic syndrome - The mutation can be detected early at diagnosis or acquired during disease progression and is associated with poor outcome. *Br. J. Haematol.* **139,** 405–414 (2007).
27. Sakurai, M. *et al.* Impaired hematopoietic differentiation of RUNX1-mutated induced pluripotent stem cells derived from FPD/AML patients. *Leukemia.* (epub ahead of print 15 April 2014; doi:10.1038/leu.2014.136).
28. Bravo, J., Li, Z., Speck, N. A. & Warren, A. J. The leukemia-associated AML1 (Runx1)-CBF beta complex functions as a DNA-induced molecular clamp. *Nat. Struct. Biol.* **8,** 371–378 (2001).
29. Akamatsu, Y., Tsukumo, S. I., Kagoshima, H., Tsurushita, N. & Shigesada, K. A simple screening for mutant DNA binding proteins: application to murine transcription factor PEBP2?? subunit, a founding member of the Runt domain protein family. *Gene* **185,** 111–117 (1997).
30. Yoshimi, A. *et al.* Evi1 represses PTEN expression and activates PI3K/AKT/mTOR via interactions with polycomb proteins. *Blood* **117,** 3617–3628 (2011).

Acknowledgements

This work was supported in part by grants-in-aid from the Ministry of Health, Labor and Welfare of Japan (H23-Nanchi-Ippan-104; M. Kurokawa) and KAKENHI (24659457; M. Kurokawa). We thank R. Lewis (University of Nebraska Medical Center) and T. Kitamura (Institute of Medical Science, The University of Tokyo) for providing essential materials; T. Koike (Nagaoka Red Cross Hospital), K. Nara (Ootemachi Hospital), K. Suzuki (Japanese Red Cross Medical Center), H. Harada (Fujigaoka Hospital), Y. Morita (Kinki University), M. Matsuda (PL Hospital), H. Kashiwagi (Osaka University), T. Kiguchi (Chugoku Central Hospital), T. Masunari (Chugoku Central Hospital), K. Yamamoto (Yokohama City Minato Red Cross Hospital), T. Takahashi (Mitsui Memorial Hospital) and T. Takaku (Juntendo University) for providing patient samples; M. Kuramitsu (National Institutte of Infectious Diseases) for providing kind support of synchronized quantitative PCR; and K. Tanaka and Y. Shimamura for their technical assistance.

Author contributions

A.Y., T.T., M.I. and M. Kurokawa analysed genetic materials and performed functional studies. A.T., H.I., M.N., Y.N. and S.A. were involved in sequencing and/or functional studies. M. Kawazu, T.U. and H.M. took part in whole-exome sequencing, deep sequencing and bioinformatics analyses of the data. A.Y., T.T., M.I., H.H., K.U., Y.H., E.I., K.K. and H.N. collected specimens. A.Y. and T.T. generated figures and tables. M. Kurokawa designed and led the entire project. A.Y., T.T. and M. Kurokawa wrote the manuscript. All authors participated in the discussion and interpretation of the data.

Additional information

Accession codes: Sequence data for FPD/AML patients has been deposited in GenBank/EMBL/DDBJ sequence read archive (SRA) under the accession code SRP043031

Supplementary Information accompanies this paper at http://www.nature.com/naturecommunications

Competing financial interests: The authors declare no competing financial interests.

Reprints and permission information is available online at http://npg.nature.com/reprintsandpermissions

How to cite this article: Yoshimi, A. *et al.* Recurrent *CDC25C* mutations drive malignant transformation in FPD/AML. *Nat. Commun.* 5:4770 doi: 10.1038/ncomms5770 (2014).

Gene Alterations Involving the CRLF2-JAK Pathway and Recurrent Gene Deletions in Down Syndrome-Associated Acute Lymphoblastic Leukemia in Japan

Isamu Hanada,[1] Kiminori Terui,[1] Fumika Ikeda,[1] Tsutomu Toki,[1] Rika Kanezaki,[1] Tomohiko Sato,[1] Takuya Kamio,[1] Ko Kudo,[1] Shinya Sasaki,[1] Yoshihiro Takahashi,[2] Yasuhide Hayashi,[3] Takeshi Inukai,[4] Seiji Kojima,[5] Kenichi Koike,[6] Yoshiyuki Kosaka,[7] Masao Kobayashi,[8] Masue Imaizumi,[9] Tetsuo Mitsui,[10] Hiroki Hori,[11] Junichi Hara,[12] Keizo Horibe,[13] Jun-ichi Nagai,[14] Hiroaki Goto,[15] and Etsuro Ito[1]*

[1]Department of Pediatrics, Hirosaki University Graduate School of Medicine, Hirosaki, Japan
[2]Department of Pediatrics, Aomori Prefectural Central Hospital, Aomori, Japan
[3]Department of Hematology and Oncology, Gunma Children's Medical Center, Gunma, Japan
[4]Department of Pediatrics, School of Medicine, University of Yamanashi, Yamanashi, Japan
[5]Department of Pediatrics, Nagoya University Graduate School of Medicine, Nagoya, Japan
[6]Department of Pediatrics, Shinshu University School of Medicine, Matsumoto, Japan
[7]Department of Hematology and Oncology, Hyogo Prefectural Kobe Children's Hospital, Kobe, Japan
[8]Department of Pediatrics, Hiroshima University Graduate School of Biomedical Sciences, Hiroshima, Japan
[9]Department of Hematology and Oncology, Miyagi Children's Hospital, Sendai, Japan
[10]Department of Pediatrics, Yamagata University School of Medicine, Yamagata, Japan
[11]Department of Pediatrics and Developmental Science, Mie University, Graduate School of Medicine, Tsu, Japan
[12]Department of Pediatric Hematology/Oncology, Osaka City General Hospital, Osaka, Japan
[13]Clinical Research Center, National Hospital Organization Nagoya Medical Center, Nagoya, Japan
[14]Division of Laboratory Medicine, Clinical Research Institute, Kanagawa Children's Medical Center, Yokohama, Japan
[15]Division of Hemato-Oncology and Regenerative Medicine, Kanagawa Children's Medical Center, Yokohama, Japan

In Western countries, gene alterations involving the CRLF2-JAK signaling pathway are identified in approximately 50–60% of patients with Down syndrome-associated acute lymphoblastic leukemia (DS-ALL), and this pathway is considered a potential therapeutic target. The frequency of *BTG1* deletions in DS-ALL is controversial. *IKZF1* deletions, found in 20–30% of DS-ALL patients, are associated with a poor outcome and *EBF1* deletions are very rare (~2%). We analyzed 38 patients to determine the frequencies and clinical implications of CRLF2-JAK pathway genetic alterations and recurrent gene deletions in Japanese DS-ALL patients. We confirmed a high incidence of *P2RY8-CRLF2* (29%) and *JAK2* mutations (16%), though the frequency of *P2RY8-CRLF2* was slightly lower than that in Western countries (~50%). *BTG1* deletions were common in our cohort (25%). *IKZF1* deletions were detected in 25% of patients and associated with shorter overall survival (OS). *EBF1* deletions were found at an unexpectedly high frequency (16%), and at a significantly higher level in *P2RY8-CRLF2*-positive patients than in *P2RY8-CRLF2*-negative patients (44% vs. 4%, $P = 0.015$). Deletions of *CDKN2A/B* and *PAX5* were common in *P2RY8-CRLF2*-negative patients (48 and 39%, respectively) but not in *P2RY8-CRLF2*-positive patients (11% each). Associations between these genetic alterations and clinical characteristics were not observed except for inferior OS in patients with *IKZF1* deletions. These results suggest that differences exist between the genetic profiles of DS-ALL patients in Japan and in Western countries, and that *P2RY8-CRLF2* and *EBF1* deletions may cooperate in leukemogenesis in a subset of Japanese DS-ALL patients.

INTRODUCTION

Down syndrome (DS) shows a significantly increased incidence of both acute myeloid leukemia and acute lymphoblastic leukemia (ALL) in childhood, and a complex relationship to leukemogenesis (Nižetić and Groet, 2012). Patients with DS and ALL have a lower incidence of favorable cytogenetic abnormalities (e.g., t(12;21) and high hyperdiploidy; Forestier et al., 2008; Maloney et al., 2010) and poorer treatment outcomes than

Supported by: Grants-in-Aid for Scientific Research from the Ministry of Education, Culture, Sports, Science and Technology of Japan; Grants-in-Aid for Cancer Research from the Ministry of Health, Labour and Welfare of Japan; Grant for Clinical Cancer Research from the Ministry of Health, Labour and Welfare of Japan.

*Correspondence to: Etsuro Ito, M.D., Ph.D., Department of Pediatrics, Hirosaki University Graduate School of Medicine, 5 Zaifucho, Hirosaki, Aomori 036-8562, Japan.
E-mail: eturou@cc.hirosaki-u.ac.jp

Received 12 May 2014; Accepted 15 June 2014
DOI 10.1002/gcc.22201
Published online 16 July 2014 in Wiley Online Library (wileyonlinelibrary.com).